AD-A136 125 RESPONSE MECHANISM: BLAST/FIRE INTERACTIONS(U) NOTRE DAME UNIV IN DEPT OF AEROSPACE AND MECHANICAL ENGINEERING A M KANURY NOV 83 EMW-C-0366 1/1

UNCLASSIFIED F/G 18/3 NL

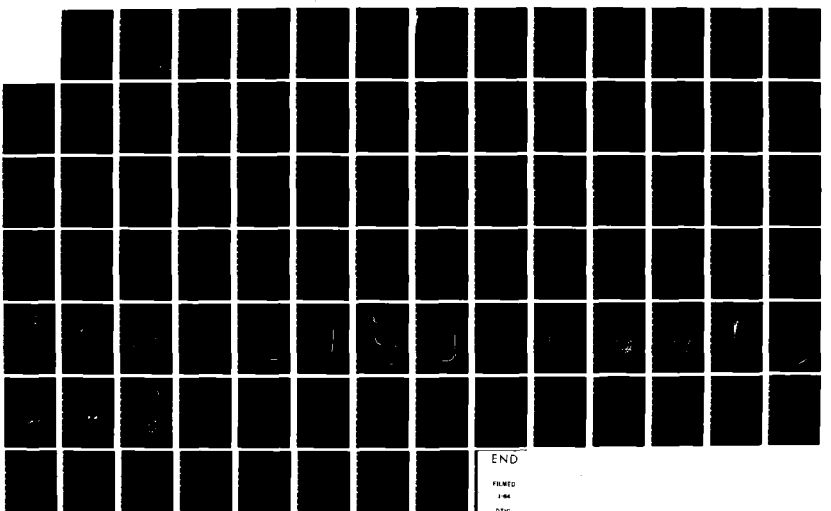

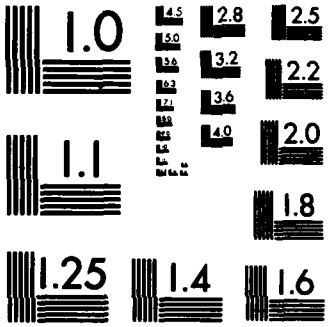

(12)

RESPONSE MECHANISM: BLAST/FIRE INTERACTIONS

Final Report
for
Federal Emergency Management Agency
Washington, D.C. 20472

Contract No. EMW-C-0366
Work Unit No. 2564 H

November 1983

APPROVED FOR PUBLIC RELEASE
DISTRIBUTION UNLIMITED

RESPONSE MECHANISM: BLAST/FIRE INTERACTIONS

by

A. Murty Kanury
Department of Aerospace and Mechanical Engineering
University of Notre Dame
Notre Dame, Indiana 46556

November 1983

Final Report
for
Federal Emergency Management Agency
Office of Research
National Preparedness Programs
Washington, D.C. 20472
Contract No. EMW-C-0366
Work Unit No. 2564 H

UNCLASSIFIED

SECURITY CLASSIFICATION OF THIS PAGE *(When Data Entered)*

REPORT DOCUMENTATION PAGE		READ INSTRUCTIONS BEFORE COMPLETING FORM
1. REPORT NUMBER	2. GOVT ACCESSION NO. AD-A136125	3. RECIPIENT'S CATALOG NUMBER
4. TITLE *(and Subtitle)* Response Mechanism: Blast/Fire Interaction		5. TYPE OF REPORT & PERIOD COVERED Final Report
		6. PERFORMING ORG. REPORT NUMBER
7. AUTHOR(s) A. Murty Kanury		8. CONTRACT OR GRANT NUMBER(s) EMW-C-0366
9. PERFORMING ORGANIZATION NAME AND ADDRESS University of Notre Dame Notre Dame, IN 46		10. PROGRAM ELEMENT, PROJECT, TASK AREA & WORK UNIT NUMBERS FEMA WU No. 2564H
11. CONTROLLING OFFICE NAME AND ADDRESS Federal Emergency Management Agency Office of Research/National Preparedness Programs Washington, DC 20472		12. REPORT DATE November 1983
		13. NUMBER OF PAGES 70
14. MONITORING AGENCY NAME & ADDRESS *(if different from Controlling Office)*		15. SECURITY CLASS. *(of this report)* Unclassified
		15a. DECLASSIFICATION/DOWNGRADING SCHEDULE

16. DISTRIBUTION STATEMENT *(of this Report)*

APPROVED FOR PUBLIC RELEASE; DISTRIBUTION UNLIMITED

17. DISTRIBUTION STATEMENT *(of the abstract entered in Block 20, if different from Report)*

18. SUPPLEMENTARY NOTES

19. KEY WORDS *(Continue on reverse side if necessary and identify by block number)*

Fires, Extinction, Blast/fire interaction, Reflashing of blownout fires

20. ABSTRACT *(Continue on reverse side if necessary and identify by block number)*

Hypotheses are formulated of the process of interaction between an airblast and fires supported by liquid fuels and wood cribs. A map of blast weakness versus fire strength is conceived on which the regime of fire extinction can be delineated from the regime where the fire sustains the blast. The fire strength is described for liquid fuels primarily by the heat of combustion; and for wood, it is mainly described by the preburn time. The concept is substantiated by the SRI shocktube data.

DD FORM 1 JAN 73 1473 EDITION OF 1 NOV 65 IS OBSOLETE

UNCLASSIFIED

SECURITY CLASSIFICATION OF THIS PAGE *(When Data Entered)*

RESPONSE MECHANISM: BLAST/FIRE INTERACTIONS

by

A. Murty Kanury
Department of Aerospace and Mechanical Engineering
University of Notre Dame
Notre Dame, Indiana 46556

September 1983

Final Report
for
Federal Emergency Management Agency
Office of Research
National Preparedness Programs
Washington, D.C. 20472
Contract No. EMW-C-0366
Work Unit No. 2564 H

RESPONSE MECHANISM: BLAST/FIRE INTERACTIONS

by

A. Murty Kanury
Department of Aerospace and Mechanical Engineering
University of Notre Dame
Notre Dame, IN 46556

The mechanism of interaction between a blast wave and a diffusion flame is studied with the objective of correlating data obtained in shocktube tests. Based on a scrutiny of the interplay between physical transport processes and chemical kinetic reaction processes, a Damkohler number P is identified to represent the inverse of the blast strength. Also identified is a fire strength parameter q which defines the fuel character. On a map of P(q), regimes in which extinction is expected are distinguished from those in which the fire will sustain the impact of the blast. Where charring fuels are involved, the role of glowing combustion in the reflashing of an extinguished flame is examined.

The hypothesis is tested with the experimental data obtained by Backovsky, Martin and McKee at SRI International to reach conclusions: (a) liquid fuel (i.e., Class B) fires are consistent with the hypothesis; (b) barricades placed upstream of the fire tend to produce recirculation of flow and as a result increase the flow residence time to enhance the stability of the fire; (c) the barricade heights for which data are now available are too small compared to the fire bed dimensions to allow attainment of systematic extinction -no extinction boundaries on the P versus q map; (d) wood-crib (i.e., Class A) fires also conform with the hypothesis including in the reflashing phenomenon, although the combustion behavior of crib fires poses numerous inherent ambiguities; and (e) shredded paper tray fires are in a class all by themselves and are unexplained by the present hypothesis.

ABSTRACT

The mechanism of interaction between a blast wave and a diffusion flame is studied with the objective of correlating data obtained in shocktube tests. Based on a scrutiny of the interplay between physical transport processes and chemical kinetic reaction processes, a Damkohler number P is identified to represent the inverse of the blast strength. Also identified is a fire strength parameter q which defines the fuel character. On a map of P(q), regimes in which extinction is expected are distinguished from those in which the fire will sustain the impact of the blast. Where charring fuels are involved, the role of glowing combustion in the reflashing of an extinguished flame is examined.

The hypothesis is tested with the experimental data obtained by Backovsky, Martin and McKee at SRI International to reach conclusions: (a) liquid fuel (i.e., Class B) fires are consistent with the hypothesis (b) barricades placed upstream of the fire tend to produce recirculation of flow and as a result increase the flow residence time to enhance the stability of the fire; (c) the barricade heights for which data are now available are too small compared to the fire bed dimensions to allow attainment of systematic extinction -no extinction boundaries on the P versus q map; (d) wood-crib (i.e., Class A) fires also conform with the hypothesis including in the reflashing phenomenon, although the combustion behavior of crib fires poses numerous inherent ambiguities; and (e) shredded paper tray fires are in a class all by themselves and are unexplained by the present hypothesis.

CONTENTS

NOMENCLATURE

A	area of transfer, also a property constant
a	stoichiometric coefficient
B	a property constant
b	stoichiometric coefficient, also stick thickness
c_0	speed of sound
C_p	specific heat
Da	Damkohler number, general definition
E	activation energy
f	stoichiometric fuel/oxidant mass ratio
h_C	enthalpy of combustion
h_D	mass transfer coefficient
k_0	prexponential factor
L	latent heat of pyrolysis
ℓ	reaction space size
m,n	orders of reaction
p	pressure
P	Damkohler number
q	dynamic pressure
q	fire strength parameter
$\dot{q}''$	fire to fuel heat flux
$\bar{R}$	universal gas constant
T	temperature
t^*	characteristic time
t°	stick burning time
u	velocity

W mass transfer rate

Y mass fraction

α thermal diffusivity

ρ density

γ ratio of gas specific heats

θ nondimensional temperature

τ charring solid fire strength parameter, nondimensional preburn time

Subscripts

A fuel

B oxidant (also denoted sometimes by 0)

c char

f flaming

G glowing

g gas phase

i initial or supply state

ℓ at coordinate = ℓ

0 at coordinate = zero

0 original solid

p pyrolysis

s surface glowing reaction

∞ ambient

LIST OF FIGURES

LIST OF TABLES

INTRODUCTION

Emanation of thermal radiation and initiation of a blast wave [1-4] are two of the early effects of the fireball of a nuclear explosion. The thermal radiation, propagating at the speed of light, impinges on various objects around the ground-zero. Ignition is possible within a critical distance in which the heat fluxes are high enough and exposures are long enough. The primary fires thus initiated are established and made to grow in intensity by a series of highly transient physico-chemical processes: the solids continue to be transiently heated; combustible gases and vapors continue to be formed by pyrolysis or vaporization; vapors mix with air; exothermic reactions in the mixture lead to evolution of the flame; and these flames propagate over the burning material.

As Backovsky et al point out [3], fire in this setting is unlike the prompt effects of a nuclear explosion in that it continues for some time to take its own course of development and spread to destroy property and life. By this course of development, it is also perhaps controllable through the available post-explosion time, although its magnitude may make the efforts to control appear futile in the wake of a nuclear attack.

There is considerable literature on radiant ignition of idealized surfaces and some on temporally distributed exposure and on nonideal surfaces. There is extensive research activity sponsored by the National Bureau of Standards [5] on the topic of fire growth in enclosures. Fire spread in the forest environment is a process relatively well-understood for the purposes of control and damage mitigation. Progress is thus being made in gaining an understanding of the fire growth behavior in the absence of blast wave effects.

As the primary fires in the open and within structures continue to grow, the blast wave arrives to perturb them. An already complicated transient fire development process is now rendered even more complex by the propagating fields of pressure and flow brought about by the blast wave. The abrupt adiabatic compression of air results in an increase in temperature. There also may be the tail-end of the thermal radiation pulse. The growing fire is thus subjected to changing pressure with winds of varying temperature with an externally imposed transient thermal pulse.

Leave alone the blast damage to structures for the moment; enough knowledge does not exist on the manner in which the blast winds perturb the nascent fires. Herein lies an important element of uncertainty in estimating the magnitude of the fires resulting from a nuclear blast. It is this element which constitutes the subject of present research.

The problem of blast interaction with fire was studied theoretically by Fendell at TRW [6] and experimentally by Martin, Backovsky and Goodale at SRI, [1-3], both under the sponsorship of FEMA. Attention here is focussed on the experimental data from the SRI shock tube facility. Data from both the shock tube facility and the scanty field tests involving high explosive simulations have resulted in a considerably improved understanding of the blast/fire interaction process. Because of cost considerations, however, the available experiments will always be limited in number, and in scope, to hamper deduction of reliable generalizations useful in FEMA's objective of damage mitigation and fire control. Experiments are necessary to identify processes and to verify theoretical hypotheses. The objective of the present work is to develop hypotheses of blast/fire interaction based on, and to be verified by, the available experiments. Since an unusual mutual imposition of physics and chemistry is involved in the problem of combustion perturbed by a blast, an account of the various variables in a systematic framework is desirable. The research reported here deals with such an account, to achieve an improved consistency among the available blast/fire interaction data, to arrive at a rational and generalizable interpretation of the observations to date, and to alleviate, at least in part, the current uncertainty in estimating the magnitude of primary fires resulting from a nuclear explosion.

There are, of course, other elements of uncertainty with which the decision-makers of emergency management have to cope. These additional facets of uncertainty stem from happenings subsequent to the arrival of the blast. The structures may, and will, respond to the blast wave soon. Windows break; room-filling ensues; loading of the walls and floors arises due to the transient overpressure pulse; they collapse by bending or by shearing; their fragments flying around; the fuel is now merely piles of debris. The scene then is probably dominated by fires in debris, apparently smoldering and dying, and yet, apparently eager to flare up. Winds continue to blow, and the residual thermal radiation is almost gone. Secondary fires arise due to electrical shorts, due to upsetting of heating elements in furnaces and kilns

and due to release of highly flammable fuel liquids and gases and other chemicals. Little is known quantitatively of this secondary fire scenario. It is also in this stage that the multiple burst effects come to be important. The work reported here does not address the secondary fire problem, nor the multiburst problem.

The general objective of this work thus is to study the mechanisms of interaction between a blast wave and such a diffusion flame as expected in connection with a nuclear explosion and as encountered in simulations employing shocktube experiments and/or high explosives field tests. The specific objective is to identify the hypotheses underlying the augmentation or extinguishment of diffusion flames by blast waves so that the expected important variables may be systematically reduced to nondimensional ratios. The existing data will then be correlated nondimensionally to explain the currently available observations and to design future experiments.

This objective is sought to be accomplished through the following sequence of steps:

(a) systematically identify the variables involved;

(b) formulate hypothetical mechanisms of flame augmentation or extinguishment;

(c) assess from these hypotheses the combinations of variables which operate cooperatively or antagonistically;

(d) derive from this assessment, dimensionless ratios embodying the mechanisms;

(e) develop correlations of the existing data by means of these dimensionless parameters;

(f) identify the most probable hypotheses of augmentation or extinguishment which appear to explain the existing experimental observations; and

(g) designate the specific data that need to be recorded in the future blast fire and shock tube experiments.

APPROACH SYNOPSIS

Considered here are fires supported by hydrocarbon liquids and cellulosic solids. Fuels are characterized by their thermal, thermodynamic, and combustion properties. The burning of cellulosic solids takes considerable time to become established, due to the relatively slow heat conduction. Furthermore the mechanism of combustible production is chemical in nature when the fuel is a cellulosic solid and physical when it is a hydrocarbon liquid. As a result of these differences, the burning process attains a steady state quickly if the fuel is a liquid and not so quickly if it is a solid. During the initial transient development phase, thus, the burning of a cellulosic fuel array becomes progressively more intense with time since ignition. In assessing the effects of any imposed perturbation on such a fire, then, the time at which the perturbation is imposed becomes an important factor. This time is here termed the 'preburn time'.

Several geometries of the burning surfaces relative to the flow induced by the blast are considered. These include: simple shear flow geometry (i.e., a flat plate parallel to the flow); stagnation geometry (i.e., a plate normal to the flow); and a combined geometry (i.e., an array of fuel cylinders arranged in the fashion of a crib). Effects of barriers, recirculation zones and other classical flame-holding systems are discussed in the light of these geometries.

The fundamental nature of burning of objects is governed by a combination of physics and chemistry [7]. The physical processes involve preparation of the fuel to a form suitable for combustion (i.e., vaporization, preheating, etc.), mixing of the reactants to form a combustible mixture, removal of products and heat from the flame zone, etc. The primary chemical process pertains to the oxidation reaction between the fuel and oxygen to form the products and to release energy. (Production of combustible gases from the fuel (especially if it were a solid) may itself be a chemical degradation process.) When the chemical processes are extremely fast compared to the physical processes, what is known as a physically-controlled flame would result. The ratio of the physical characteristic time to the chemical characteristic time (or, simply the chemical rate to physical rate) is known as Damkohler number, Da. When Da is very large, a well-established physically controlled flame exists. Any changes caused by the blast wave in the pressure, velocity and the temperature fields will alter the relative roles

played by chemistry and physics in the governance of the flame behavior. When the Damkohler number is made sufficiently low by the blast wave, the chemical processes become too slow compared to the accentuated physical processes and the consequence is an extinguishment.

Whereas the Damkohler number plays a dominant role in the response of a flame to the impact of a blast wave, other factors may intrude to modify the behavior. Barriers and other recirculation devices, for example, prolong the physical residence of the reactants in the reaction zone. This prolonged residence corresponds to the slowing down of physical processes. In conjunction with a chemical reaction of a specified characteristic speed, the slowed physical processes result in an increase in Da. If this increase is sufficiently large, the flame will become resistant to blow off. One can easily write down the equations of unsteady conservation of mass, momentum, energy, and species for the boundary layer combustion process with the appropriate boundary and initial conditions [8]. An examination of these equations, without actually solving them readily results in a set of dimensionless criteria useful in correlating the observed ignition and extinction behavior of the flames.

The approach used here is to examine the existing fire extinguishment/ augmentation data in the light of different plausible mechanisms of extinguishment, blow-off, rekindling, augmentation and alteration of the flames by blast waves. The excercise will be iterative in nature in that the postulated mechanisms attempt to explain and correlate the data while the data and observations direct towards identifying the plausible mechanisms.

PREPARATORIES

What is a Blast Wave?

The generation of a pressure wave due to rapid energy release is called an explosion [4]. When a 0.5 kg sphere of TNT (whose volume is about $3x10^{-4}$ m^3) is activated, about $3x10^{-1}$ m^3 of combustion gases at about 4 000 K and 100 000 atm are rapidly produced. These high pressure, high temperature gases isentropically expand to 'shock up' the surrounding compressible gas, namely the air. A spatial, (generally moving), discontinuity known as a shock front is thereby formed, across which pressure, temperature and density exhibit abrupt jumps. Passage of the shock front through an otherwise still air causes air to move, thus producing a particle velocity. The speed of winds thus induced is frequently expressed as a dynamic pressure. The quantity of, and the rapidity with which, energy is released by the source determines the intensity of the shock front, i.e., shock velocity, peak over pressure, dynamic pressure, temperature rise, etc. As the shock wave encounters obstacles in the course of its propagation, it is partially reflected (to augment the overpressure) and partially diffracted around the obstacle (imparting some of its energy to the obstacle). One of the consequences of this diffraction is the evolution of a recirculating (or vortex) flow on the downstream side of the obstacle.

Books on gas dynamics present a quantitative description of the shock propagation in various media. Glasstone summarizes the relevant relations for nuclear explosions in Reference 4.

Near time equal to zero, the fire ball produced by an explosion is such that pressure is high near its edge and is progressively smaller as its origin is approached. Upon expansion of the fire ball, the overpressure starts to decay so that after a certain time, the pressure behind the shock falls to the ambient pressure. At subsequent times, a partial vacuum is formed behind the shock front. This is called the negative phase. While winds blow in the direction of the shock front propagation during the duration of the positive phase , they blow towards the source during the negative phase. The steady decay of the peak overpressure with time (or distance traversed by the shock) is presented in Fig. 3.72 of Ref. 4. As the peak overpressure, the positive phase duration as well as the negative phase intensity and duration are dependent upon the distance travelled by the shockwave. While peak

overpressure is an indicator of blast intensity, dynamic pressure ($\rho u^2/2$) is an indicator of the wind velocity u. (ρ is air density behind the shock). Peak dynamic pressure also decays with increasing distance from the source.

The peak overpressure decay (when coupled with appropriate scaling laws for the source strength and height of burst* and with the following gas dynamic relations from Reference 4) leads to estimation of a variety of blast characteristics of relevance in the current study.

$$u_{shock} = c_o\left[1+\frac{\gamma+1}{2\gamma}\frac{p}{p_0}\right]^{1/2}$$

$$u_{particle} = \left(\frac{c_0 p}{\gamma p_0}\right)\left[1 + \frac{\gamma+1}{2\gamma}\frac{p}{p_0}\right]^{-1/2}$$

$$\rho = \rho_0\left[1+\frac{\gamma+1}{2\gamma}\frac{p}{p_o}\right]/\left[1+\frac{\gamma-1}{2\gamma}\frac{p}{p_0}\right]$$

$$q = \left[\frac{p^2}{2\gamma p_0}\right]/\left[1+\frac{\gamma-1}{2\gamma}\frac{p}{p_0}\right]$$

$$p_{reflected} = 2p + (\gamma+1)q$$

where P_0, ρ_0 and c_0 are respectively the ambient air pressure, density and speed of sound. p is peak overpressure, γ is ratio of specific heats ($\approx$1.4 for air), u is velocity, ρ is density, q is dynamic pressure, and $p_{reflected}$ is reflected overpressure (for normal incidence on a flat surface).

The energy released at the explosion source is distributed among a variety of modes. These modes include, first, the hot products of explosion thermally radiate to the surroundings in a characteristic pulse [4]. Second, the expanding hot gas performs mechanical work on the air to produce and propagate the shock wave (which itself imparts part of its energy to raise the kinetic energy of air by producing winds which would eventually be

* The primary scaling consideration is that, for a given peak overpressure or dynamic pressure, the height of burst, distance from ground zero, time of blast arrival, and the duration of positive phase, are all proportional to the cube-root of the weapon-yield (which is generally expressed in units of kiloton TNT equivalence).

dissipated). Furthermore, the isentropic compression of air results in a temperature rise. The sensible energy increase associated with the temperature rise is irrecoverably lost. A part of the energy involved in the winds and static pressure will be imparted to fragments of debris formed from the break up of objects in the path of the blast wave; these fragments gain kinetic and potential energies while being physically displaced through significant distances. The bursting of objects, loaded by the blast to form the fragments is itself a process in which energy is absorbed to result in strain and rupture.

What is a Fire?

Strongly exothermic oxidations constitute the bulk of combustion reactions. These reactions may occur in the gas phase, at the solid surface or within a porous solid to result respectively in flaming, glowing and smoldering. Heating of the fuel, first by an external means and then by the energy release by combustion, to produce combustible vapors, is a predominant feature of the combustion of solids and liquids. While liquid fuel fires are known as Class B fires, those of wood-like charring solids are known as Class A fires. A fire, in a broad sense, is a collection of flames generally accompanied, in Class A systems, by glowing as well as smoldering. If the fuel were supplied independently in gaseous state, the flame character will be, by and large, externally controlled. If the fuel otherwise is supplied as a liquid or solid, the flame feeds some of its energy back to the fuel source to produce combustibles at such a rate as to maintain a self-imposed pseudo-equilibrium in its characteristics. The workings of the flame in both these cases involve such component processes as mixing of the fuel vapor with air, preheating the mixture, supporting the combustion chemical reaction, and dispersing the energy and product species released in the reaction. In a flame, these processes are generally consecutive rather than simultaneous. As a consequence, the slowest of these process steps governs the overall behavior of the combustion.

Generally, combustion in fires is governed by the physics of fuel generation, mixing, and heat transfer rather than by the relatively faster chemical kinetics. In flames near extinction, however, the chemical reaction kinetics are slowed down to a speed closer to that of the physical transport pheomena. This issue will be further discussed in a later section.

Class B Fires:

Ignition of liquid fuel fires involves preheating the fuel to produce a sufficient quantity of vapor which, when mixed with air under the specific fluid dynamic mixing conditions, yields a mixture above the lean ignitibility limit. The introduction of an ignition source (a pilot flame, spark, heated wire or an incandescent particle) then produces a flame which propagates over the entire available liquid surface. This flame will soon establish itself over the liquid fuel, first going through a short transient period in which the liquid is heated to steady state, and then in a steady state. The liquid surface is usually not hotter than the saturation temperature corresponding to the ambient pressure. For most of the common liquid fuels, this boiling-point temperature is relatively low. If hot metal rims, incandescent particles or other ignition sources are absent, then a blown-out flame remains blown-out even if the mixture conditions are suitable. Note, however, that a flame may either be blown away by a blast impingement, or be simply displaced down-stream. A displaced flame can reflash to the fuel source as vapors continue to be produced and as the blast effects subside.

Consider, as shown in Fig. 1, a steadily burning pool of liquid fuel. Fig. 1a indicates the pool burning in quiescent air while 1b shows one burning in flowing air. Radiative and convective heat transfer from the flame to the fuel surface causes evaporation to provide combustible vapors to the flame. Air (oxygen) is transported to the flame from the surroundings to react with the fuel. All the reaction products and most of the heat produced are convected out of the flame; part of the energy is also radiated away.

Typical composition and temperature profiles are indicated in Fig. 2. The gas phase combustion chemistry is assumed to be infinitely fast in Fig. 2a compared to the physical processes of mixing and transfer of energy, species and momentum. Under this assumption the flame is a plane of zero thickness at which the reactants undergo combustion as fast as they are transported to it. The dominant feature of this sort of infinite rate chemistry is that the oxygen and fuel are prevented from penetrating through the flame. This is known as an ideal diffusion flame. Its characteristics are obtainable through an analysis of the associated fluid mechanics problem without regard to the chemical reaction kinetic detail. A further elaboration of this will be given in a later section.

If one tampers with the problem of Fig. 2a either to reduce the chemical reaction rate or to enhance the physical transport rates, the flame sheet ceases to be infinitesimally thin, reactants may now coexist and the flame temperature is lowered as depicted in Fig. 2b. Upon thus sufficiently broadening due to the vigorous transfer mechanisms, the flame would altogether be blown out. This extinguishment process will be further discussed later since it has a bearing on blast/fire interaction.

Class A Fires:

Wood is a member of cellulosic solid fuel family which undergoes charring combustion. Production of combustible gases (and vapors) upon heating wood is a chemical degradation process. Also known as pyrolysis or charring, this mode of thermal response of the solid fuel is in contrast with the physical (thermodynamic) evaporation of a liquid fuel.

As the combustible gases produced in the pyrolysis exit from the solid to the gas phase, they form a mixture with air in the boundary layer adjacent to the solid. This mixture may be ignited either spontaneously or by a pilot source. Even after such an ignition, continued burning may not be possible without an external heat flux to the solid. The reason for this is that energy is continuously conducted away into the interior of the solid and radiated out to the surroundings; a feeble nascent flame can not quite provide sufficient energy for these conductive and radiative drains as well as the energy required for the continuation of pyrolysis. Upon continued external heating, however, a stage soon arrives at which self-sustained burning is possible.

When the cellulosic fuel described above is a pile of sticks of wood, mutual interactions among the different fuel elements (i.e., sticks) in conserving energy would tend to aid sustained burning. The longer the burning, the more established the fire would become.

It is important to note that the surface temperature of burning wood is significantly higher than that of a typical burning liquid fuel. If the flame were to be blown away momentarily for whatever reason, the thermal inertia of the solid sustains the pyrolysis and the hot surface is capable of piloting a reignition. Additionally, if the flame were to be blown out or if it were so defective in structure as to permit penetration of oxygen to the hot surface, glowing combustion may ensue.

The role of glowing combustion will be further discussed elsewhere in this report. Suffice it to note that glowing is expected to present a substantial energy source at the surface. Enough of the energy produced in this surface-glowing will be transmitted to the solid to keep the pyrolysis continued and to thus keep combustible supply to the gas phase continued. The glowing char surface is generally capable of reigniting the gas mixture thus formed following the blowing away of the original flame. Herein lies a major difference between the burning of solids and liquids.

Control by Physics or Chemistry?

As pointed out above, the burning of any fuel involves both physics and chemistry. The physical processes involved are heat, mass and momentum transport, thermal radiation and thermodynamics. The oxidative process is chemical. To delineate the relative roles of these physical and chemical processes, consider two infinite parallel plates separated by a distance ℓ as shown in Fig. 3. Let one of these plates be the source of fuel vapor A while the other is the source of the oxidant B. Let Y_{AO} and $Y_{B\ell}$ be the mass fractions of A and B near the sources. As A and B diffuse into the space between the plates, chemical reaction will ensue.

The physical rate of transfer of the reactant species from the source to the reaction space occurs in proportion to the difference in mass fraction, the proportionality constant being the mass transfer coefficient which is a function of the flow characteristics of the reacting medium, the diffusion coefficient and density of the species through the reacting mixture and the characteristic dimension of the transfer surface. Focussing attention on the fuel species for convenience,

$$\dot{W}_A = h_{DA} A (Y_{AO} - Y_A) \qquad (1)$$

where $\dot{W}_A$ is the mass of species A transferred per unit time (kg/s), h_{DA} is the mass transfer coefficient ($kg/m^2 s$), A is the area of plate (m^2), Y_{AO} is the species A mass fraction at the source and Y_A is the same in the reaction space. The mass transfer rate for the oxidant can similarly be written as

$$\dot{W}_B = h_{DB} A (Y_{B\ell} - Y_B) \ . \qquad (2)$$

By stoichiometry $aA + bB \rightarrow$ products, the rates are related by

$$\dot{W}_B = \left(\frac{b}{a}\right) \dot{W}_A \tag{3}$$

The chemical kinetic rate is generally of the form

$$W_A = k_{OA}\, A\ell\, Y_A^{\,n} Y_B^{\,m} \exp(-E/\bar{R}T) \tag{4}$$

where k_0, n, m and E are the reaction kinetic parameters known respectively as the prexponential (collision) factor, order of the reaction with respect to fuel A and to oxidant B and activation energy. $\bar{R}$ is the universal gas constant. T is the reaction space temperature assumed here to be a prescribed constant. The above four equations can now be solved for the four unknowns: the reaction space concentrations Y_A and Y_B and the rates of consumption $\dot{W}_A$ and $\dot{W}_B$. Specifically,

$$Y_A = Y_{AO} - \left(\frac{\dot{W}_A}{A h_{DA}}\right) \tag{5}$$

$$Y_B = Y_{B\ell} - \left(\frac{b}{a}\right)\left(\frac{h_{DA}}{h_{DB}}\right)\left(\frac{\dot{W}_A}{A h_{DA}}\right) \tag{6}$$

$$\left[Y_{AO} - \left(\frac{\dot{W}_A}{h_{DA}A}\right)\right]^n \left[Y_{B\ell} - \left(\frac{b}{a}\right)\left(\frac{h_{DA}}{h_{DB}}\right)\left(\frac{\dot{W}_A}{h_{DA}A}\right)\right]^m = \left[\frac{h_{DA}A}{k_{OA}A\ell}\exp\left(\frac{-E}{\bar{R}T}\right)\right]\left(\frac{\dot{W}_A}{h_{DA}A}\right) \quad . \tag{7}$$

For given values of n, m, Y_{AO}, $Y_{B\ell}$, $(h_{DA}/k_{OA}\,\ell\,\exp(-E/\bar{R}T))$, (b/a) and (h_{DA}/h_{DB}), Eq. (7) can be solved for $(\dot{W}_A/h_{DA}A)$ and then Eqs. (5) and (6) give Y_A and Y_B. The general solution is tedious and obscuring. In order to elucidate the general features of the solution, consider n = 1 and m = 0. Then

$$Y_A = Y_{AO}\,\frac{1}{1+Da} \tag{8}$$

$$\dot{W}_A = Y_{AO}\,\frac{Da}{1+Da}\,h_{DA}A = Y_{AO}\,\frac{1}{1+Da}\,k_{OA}A\ell\,\exp(-E/\bar{R}T) \tag{9}$$

where

$$Da \equiv \frac{k_{OA}A\ell\,\exp(-E/\bar{R}T)}{h_{DA}A} \tag{10}$$

Consider now two extreme cases when Da >> 1 and Da << 1. Da is much greater than unity when the chemical reactions occur very rapidly compared to physical transfer of species. Equations (8) and (9) then reduce to $Y_A \approx (Y_{AO}/D) \approx O$(since the mass fraction can at best be equal to unity) and $\dot{W}_A \approx h_{DA}^A Y_{AO}$. Since the chemical kinetics are infinitely fast, the comparatively slower transport physics governs the global characteristics of the problem. That is, the chemical reaction consumes the reactants wherever the stoichiometric requirements are fulfilled as soon as they are brought into the reaction zone. Since the transport rates are low, the driving forces for transfer tend to be maximized as reflected by the strong spatial gradients (of the species mass fraction in this illustration). The so-called 'sudden death kinetics' culminate in the reaction at a distinct site to which the fuel and oxidant are supplied in stoichiometric proportions.

Said to be physically (or diffusionally) controlled combustion, this limiting behavior is depicted in Fig. 3. The flame located at station marked 1 is an infinitesimally thin imaginary sheet. This sort of an ideal diffusion flame arises whenever high temperatures and pressures, large reactor dimensions, low fluid velocities and low species diffusivities are encountered. If Da were not infinity but still large, the fuel and oxidant may not coexist at any station; as a result, the flame ceases to be a sheet of zero thickness. Said differently, finite rate chemistry broadens the flame (between stations labelled 2 and 3 in Fig. 3). Chemistry in these nonideal diffusion flames can not be altogether ignored in attempts to arrive at the combustion characteristics.

Consider now the second limiting case when Da << 1. This situation signifies that the chemical reaction rate is extremely small compared to the physical transport rates. Low temperatures and pressure, small physical dimensions of the reactor, greatly enhanced flow and mixing conditions are conducive to this situation. Setting D = 0, Eqs. (8) and (9) yield $Y_A \approx Y_{AO}$ and $\dot{W}_A \approx k_{AO}^{A\ell} Y_{AO}^n Y_{B\ell}^m \exp(-E/\bar{R}T)$. The relatively slower chemical kinetics govern the global characteristics of this limiting combustion while the relatively fast fluid dynamic, thermodynamic and transfer processes become irrelevant simply by washing out the spatial gradients. A distinct reaction zone (i.e., flame) does not exist. This kinetically controlled oxidation process is also depicted in Fig. 3 through the spatially uniform composition profiles.

Comments

(a) In the preceding discussion, we have deliberately kept the reactor temperature fixed to develop the concept of chemical and physical control of the combustion process. A relaxation of this artificial restraint leads to an interesting explanation of the ignition and extinction phenomena relevant to the blast/fire interaction. We will carry this relaxation in the following chapter.

(b) The general descriptive results of the above analysis are valid for all values of n and m, the orders of the reaction with respect to the fuel and the oxidant.

(c) The nondimensional parameter Da is known as Damkohler number. In the preceding discussion, it is defined as the ratio of characteristic chemical reaction rate to the physical supply rate of species A. It could also have been defined on the basis of species B, product species, or energy. These various definitions will be related through the stoichiometry. The physical rate appearing in the denominator of any of these definitions may be based on molecular diffusion, convective transport, turbulent diffusion, or, simply, the flow rate. The Da values obtained by these various physical rates are mutually related through the thermo-fluid mechanical relations among the different physical transport quantities. No matter the specific details of definition, the Damkohler number is always a ratio of the chemical speed to physical speed, always indicating the relative magnitudes of chemical to physical rates.

EXTINCTION AND IGNITION

Of concern in this work is the behavior of fires over liquid fuel pools and wood fuel cribs upon which a blast wave is imposed. We will discuss in this chapter the interaction of a blast with liquid fuel pool fire and then extend the treatment to a wood crib fire which involves pyrolysis and glowing in addition to gas phase flames.

Pool Fire:

Consider a steadily burning pool fire shown in Fig. 1a. As a blast wave is impinged on this fire with its attendant perturbations in wind, pressure and temperature, the flame will be disturbed. Such a disturbance may manifest in one or more of the following physico-chemical phenomena.

(a) Annihilation of spacial gradients of species, temperature and velocity by the increased molecular and turbulent transport can lead to intense mixing and dilution of the reactants. Also brought about is thermal dilution and a consequent reduction in the temperature of the reaction space. The net overall effect is to reduce the Damkohler number.

(b) Energy feedback from the flame to the condensed phase fuel will be reduced due to physical displacement or deformation of the flame. This reduction would result in a decrease in fuel vapor supply to the gas phase. The consequent decrease in fuel vapor concentration may reduce the chemical kinetic rate to yield a diminished Damkohler number. A displaced or deformed flame could also be cause for a reduction of the temperature of gas phase near the fuel bed, thus accentuating the decrease in Da.

(c) Energy feedback to the fuel bed could be augmented by the wind bringing the flame closer to the surface. A higher wind velocity would then reduce the boundary layer thickness and flame stand-off distance to increase the heat transfer. This effect can be expected only when the wind is feeble. The overall result is an augmentation of the fire intensity by the imposition of the blast. This effect is contrary to that discussed in item (b) above.

(d) Energy feedback to the fuel bed will be enhanced due to the flame holding in the recirculatory zones of a baffled-barrier-flow. The barrier could be the rim of a fuel pan or simply a step located upstream of the pool.

(e) The fuel bed may be mechanically disturbed and dispersed by the blast wave. Such dismemberment, dispersion and redistribution of the fuel bed may,

under some conditions, increase the fire intensity by transforming the bulk fuel confined in a tray into an unconfined spray. Under other conditions, however, fragmentation of the fuel bed might aid to dissipate the energy content of the fuel in the tray to an ineffectually low average level. In the first situation, the dispersion to form a spray would enhance the transfer surface area available for fuel vaporization. Energy interaction among fragments of fuel is significant. In the second situation, the same increase in transfer area will make the fuel fragments lose energy to the air flow because the mutual interactions are minimal. Although significantly strong blasts are expected to produce the second situation, precise delineation of the rare conditions required to accomplish this is not easy. It appears that one can expect the first situation almost always in practical blast/fire interaction conditions.

(f) Pressure change will result in a shift in combustion chemical kinetics. By and large, combustion of hydrocarbons in air is approximately a second order reaction. As a result, the kinetic rate is proportional to the square of pressure, so that the Damkohler number increases with increasing pressure. The increase in pressure also alters the fluid dynamics to increase the coefficients of heat and mass transfer, so that the Damkohler number is reduced. The net effect of these two opposing effects of increased pressure can not be predicted without a detailed study of the underlying basic coupled phenomena. Note, however, that the pressure rise associated with a blast wave is temporally variant. As a result, arguments based on static imposition of a pressure rise might become invalid in the dynamic behavior of the blast-impacted flame.

(g) The shockwave also brings with it a temperature rise due to isentropic compression of air. This, too, is a transient phenomenon. It can be expected to have some effect on the flame especially in its chemical kinetic aspects.

(h) In all practical situations of blast wave generation by the explosion of a weapon, a thermal radiation pulse is involved [4]. The effect of the residual radiant pulse is to contribute to vaporization of the fuel bed even when the energy feedback is mitigated from the displaced or disappeared flames. Even more important is the thermal radiation pulse from subsequent weapon bursts in a multiburst scenario. The effect of a radiation pulse is altogether ignored in the present work.

By and large, most of the effects discussed above can be condensed to the following three global alterations brought about by the impingement of a blast on a flame: first, the gas phase reaction domain (which was occupied by the

flame prior to blast arrival) suffers excessive thermal dilution; second, the fuel vapor concentration in this domain is diminished; and third, oxygen concentration of the domain is increased. The first and second items dominate in determining the fate of the flaming. The flame is generally blown out completely or displaced to a downstream location. The hot fuel layer in the condensed phase loses heat to the gas phase by convection and to the interior of the fuel bed by conduction/convection. The temperature of both the gas phase and the fuel bed decrease gradually and monotonically with time; so also does the gas phase fuel concentration. If the blast effects subside before the thermal and species dilution reach critical limits, the fire may reflash or reignite. To find these critical limits is the objective of the following simple analysis.

Analysis:

The interaction process can be studied rigorously by solving the equations of conservation of total mass, momentum, energy and species under the constraints of known boundary and initial conditions along with the supplementary relations pertaining to turbulence, saturation thermodynamics, ideal gas law, laws of gas mixtures, transport laws, chemical reaction kinetics, energetics and equilibria and stoichiometry. These general conservation equations are available in combustion textbooks. All combustion problems are but special cases described by these equations. With respect to ignition and extinction, one seeks solutions for the problem in which energy and species concentrations are so disturbed by the flow, to cause large and abrupt temperature rise (ignition) or decrease (extinction). Due to the inherent nonlinearities in the governing equations only numerical solutions are generally possible although some asymptotic solutions of the limiting cases are in existence. In the following, a simple algebraic analysis is presented to obtain a closed-form solution of the reacting flow problem. This solution clearly depicts the ignition and extinction phenomena.

Suppose that Y_{Ai} is the mass fraction of the fuel at the supply boundary into the reacting gas phase in which the mass fraction is Y_A. If the average reaction rate is $(-\dot{W}_A''')$ kg/m^{3}s, the characteristic reaction time, t*, is of the order

$$t^* \sim \frac{\rho(Y_{Ai}-Y_A)}{(-\dot{W}_A''')} \qquad (11)$$

The reaction rate may be written as

$$-\dot{W}_A''' = k \rho Y_A \tag{12}$$

$$k \equiv k_0 \exp(-E/\bar{R}T) \tag{13}$$

where the reaction is taken to be of first order for illustrative purpose. k is the specific reaction rate constant (units 1/sec). k_0 is the preexponential collision factor (units 1/sec), E is activation energy (J/kgmole), $\bar{R}$ is the universal gas constant (J/kgmole K); and T is the characteristic temperature (K) of the reaction system. ρ is the density reacting mixture, (kg/m^3), a function of the pressure, temperature and composition of the reacting gas phase. Combining Eqs. (11) and (12) the fractional destruction of fuel species by combustion is given by

$$\frac{Y_{Ai}-Y_A}{Y_{Ai}} = \frac{kt^*}{1+kt^*} \tag{14}$$

t* is to be equal to the time provided by physics. As such, it may be expressed in various ways. It can be the reaction volume (V) divided by the volumetric flow rate of reactants ($\dot{V}$). It can also be the ratio of reaction path length (ℓ) to the flow velocity (u). Equally well, it can be the length ℓ squared over the diffusion coefficient. Other ways of defining the time are also suitable. Thus, Eq. (14) is merely the species conservation principle in which the term kt* corresponds to the ratio of chemical reaction rate to a physical rate (i.e., diffusion rate, convection rate, etc.) The energy conservation, similarly, is given by

$$\frac{Y_{Ai}-Y_A}{Y_{Ai}} = \frac{C_{pg}(T-T_i)}{Y_{Ai}h_c} \tag{15}$$

Where C_{pg} is the gas phase specific thermal capacity (J/kg K), T_i is the source, reference, or initial temperature and h_c is enthalpy of combustion (J/kg $_{fuel}$). The origin of Eq. (15) is, in fact, a combination of the species A and energy conservation equations between which the nonlinear reaction terms can be eliminated by Schvab-Zeldovitch transformation [7,8] involving the definition of a composite variable $[h_c Y_A + C_{pg} T]$, conserved under the usual convective diffusion constraints.

From Eqs. (14) and (15) one can now obtain

$$\frac{C_{pg}(T-T_i)}{Y_{Ai}\ h_c} = \frac{kt^*}{1+kt^*}$$

so that with Eq. (13),

$$P = \frac{e^{1/\theta}(\theta-\theta_i)}{q-(\theta-\theta_i)} \tag{16}$$

where, with $t = \ell/u$ = the time taken by the flow of velocity u to traverse a lengh ℓ,

$$\theta \equiv \bar{R}T/E \qquad \theta_i \equiv \bar{R}T_i/E$$

$$P \equiv k_0\ell/u \qquad q \equiv \bar{R}h_c Y_{Ai}/EC_{pg}$$

The quantity P is a Damkohler number. q is indicative of the energetic strength of the reaction. θ_i is the initial or boundary temperature normalized with the reaction activation temperature. Whereas q gives a measure of energy release quantity, the nondimensional activation energy $(1/\theta_i)$ gives a measure of the temperature-dependency of the combustion reaction.

In Figure 4, a sketch of Eq. (16) is given to demonstrate the general character of θ dependence of P for any given values of q and θ_i. The curve is generally s-shaped. The lowest branch of this curve, insensitive to both P and q, corresponds to the extremely slow oxidation reactions and is known as the 'frozen' branch. As one increases the chemical reaction rate, P increases and minute temperature rise will result. Upon thus reaching the state identified by I, Eq. (16) says that the reaction system has to follow the course represented by the broken line in Fig. 4. This course, however, is physically forbidden since it implies that a decrease in reaction rate or an increase in physical dispersion rate (both of which make P fall) would increase the reaction temperature. The only physically allowed recourse for the reaction process then is to experience an abrupt jump from state I to state I' on the high temperature branch of the solution which stands for the equilibrium combustion resulting in a flame. This abrupt jump is known as ignition.

Consider now a flame already existent somewhere on the equilibrium branch of the solution. As this flame is so perturbed by external action as to reduce P either by decreasing the numerator involving the characteristic chemical kinetic rate or by increasing the denominator involving the characteristic physical transport rate, the flame temperature gradually diminishes until state E is reached. From state E, the system is asked to enter the forbidden branch. As a result, it jumps abruptly from E to E' on the frozen branch, this jump being associated with what is known as extinction.

A branch of applied mathematics known as catastrophe theory evolved over the last two decades to describe the abrupt jump processes of this sort as they arise in the fields of chemical engineering, biology, elasticity, and disaster management. Problems involving jump processes in these fields are generally not amanable to solutions by the classical methods of mathematics of continuous functions.

Having thus described the general nature of the solution, we present in Figs. 5-8 the parametric dependency of the solution. Figure 5 indicates that the hysterisis between II'EE' discussed above is not apparent when the activation energy is low, for then the temperature-dependence of the reaction rate is rather weak. (Recall that θ, θ_i, and q all become large as E becomes small). The reaction temperature in this circumstance increases with an increasing Damkohler number monotonically although an inflection point is exhibited in this relation. The thermochemical intensity of the reaction (q/θ_i) has a significant effect on the temperature attained by the reacting system.

For $\theta_i \leq 0.25$, the catastrophies of ignition and extinction are evident. A comparison of Figs. 6, 7a, and 8 indicates the effect of activation energy ($1/\theta_i$) on the shape of the curves. The ignition Damkohler number is higher for higher activation energy at any q/θ_i and is relatively insensitive to (q/θ_i) at any activation energy ($1/\theta_i$). More drastic, however, is the arrival of extinction. A high activation energy flame is prone to be extinguished more abruptly as evidenced by the relatively increasing steepness of the equilibrium branches as the activation energy is increased. Additionally, the higher the activation energy, the higher the extinction Damkohler number.

A comparison of Figs. 7 a-c shows the influence of the fire strength parameter q on ignition and extinction phenomena in a much greater detail than, but quite consistent with, Figs. 6 and 8. Energetically weaker flames are more abrupt in their response to perturbations aimed at extinction. Weaker flames are prone to be extinguished at a larger Damkohler number. The ignition process however, is only weakly influenced by variations in q/θ_i.

This last observation is of immense importance in blast/fire interaction studies. For the case of medium activation energy ($1/\theta_i = 40$), Fig. 9 shows the ignition and extinction Damkohler numbers as dependent upon the energetic strength q/θ_i of the flames. The relative insensitivity of ignition is obvious. More importantly, the extinction process is strongly dependent on the flame's energetic strength.

One can view the graph of Fig. 9 as follows. Flames and perturbations falling in the area under the extinction curve correspond to situations in which extinction is imminent; those falling in the area above the curve are immune to extinction. Energetically weak flames (i.e., q is low) impacted by strong blasts (i.e., P is low), for instance, fall near the origin of the graph and are subject to extinction. Energetically robust flames impacted by weak blasts, on the other hand, fall far away from the origin and are expected to survive the blast. Viewed in another way, corresponding to any given fire strength (q/θ_i) there exists a lower limit blast strength (upper limit P) below which extinction is not possible. For example, if $q/\theta_i = 20$, ℓn P can not be lower than 3.5 if extinction is to be impossible. Alternately, corresponding to any given blast strength, there exists a lower limit flame strength beyond which extinction is impossible. As an example, for a blast whose strength is described by ℓn P = 8, fires energetically stronger than those represented by $q/\theta_i = 7$ are capable of resisting extinction.

An important point has to be made here as strongly as possible. In the above analysis, a global mechanishm is postulated for the interaction between a flame and a blast wave. By mere algebraic manipulation of the species and energy conservation priciples, the concepts of ignition and extinction are developed. The precise gas phase chemical reaction mechanisms are not always fully known. As a result, global kinetics are employed. There also exists a need to define the physical rate appearing in the denominator of Damkohler number. This physical rate may be a composite of both diffusion and convection. The exact and precise relation of Eq. (16) (and Fig. 4) is obtainable only by completely solving the total conservation equations of mass, momentum, energy, and species with appropriate boundary conditions. This solution will most probably require numerical computations due to the strong nonlinearities involved.

The simple exposition presented above is sufficient, to develop a methodology to correlate the existing experimental data, as shown in the following chapter.

Charring Solid Fire:

Consider a piece of wood burning in a fire, most generally in the company of other similar pieces. Combustion of wood involves at least two distinct phases: flaming and glowing.

The flaming process is not unlike that of liquid fuels. The prime difference lies in the method of production of combustible gases. Whereas in the burning of a liquid fuel the fuel vapors are evolved by a thermodynamic evaporation process , they are produced by an irreversible thermal chemical degradation process in wood burning. While liquid vaporization is a surface process with a preheated liquid layer under the vaporizing surface, the solid pyrolysis is a distributed volumetric chemical kinetic process. In liquid vaporization, the mass transfer results in a regressing surface. In wood pyrolysis, the exposed surface is stationary during the flaming combustion phase. If excessive gas flow velocities are involved, erosion and ablation may result to make the exposed surface regress with time. ; but these high velocities blow the flame away to initiate glowing. In liquid burning, as the evaporating surface regresses, the subsurface preheated layer also regresses at the same speed into the liquid, thus maintaining a temperature field in the liquid unaltered in time in the frame of coordinates fixed on the regressing surface. This temporal invariance of the condensed phase heating does not hold for woodburning, in which solid phase transient conduction continuously and contiguously tends to even out the temperature gradients. Upon continued flaming combustion of wood, a carbonaceous char layer is formed near the surface. This layer is altogether devoid of capacity to further pyrolyze. Pyrolyzates are then produced within the solid; they flow out of the solid through the char sheath, mix with air in the gas phase, combust and produce the flame. The surface char layer grows in thickness progressively as the pyrolysis process penetrates into the interior of the solid. Based on the knowledge of transient conduction process, it can be shown that the temperature gradients are steepest near the exposed surface and that, the pyrolysis zone becomes progressively broader as the solid is gradually charred away. If the solid is finite in thickness, a time will arrive at which the entire body is converted to char; no more gas phase pyrolyzates can be produced; flaming ceases.

The differences between liquid and solid fuels undergoing flaming combustion as described above are important in our attempts to sort out the blast/fire interactions. In the early stages of wood burning, the pyrolysis layer is yet to be established in its inward progress into the solid; the longer the heating and burning in these initial stages, the more sustained the flames would become.

As long as the flames cover the burning solid surface, the oxygen concentration at the solid surface is minimal or zero. If the flame is ideally diffusion-controlled, oxygen can not penetrate to the fuel-side. On the other hand, if finite-rate gas phase combustion kinetics are involved or if the flame is mechanically ruptured, then oxygen can reach the hot solid surface. Glowing combustion of the carbonaceous solid residue (viz: the char) is then expected.

Glowing combustion of carbonaceous solids involves five main steps in series: diffusion of oxygen to the hot surface, adsorption of this oxygen by the surface, reaction of the adsorbed oxygen with the solid to form adsorbed product(s), desorption of the product(s), and diffusion of the desorbed product to the gas phase. The slowest of this series of steps governs the global combustion intensity. The reaction in the absorbed state can be expressed as: $C(s) + O_2 \rightarrow CO_2$.

Upon closer scrutiny, some investigators propose a slightly different mechanism, in which oxygen does not ever reach the surface. As CO_2 is formed in a thin blue flame in the gas phase, a part of it diffuses to the solid, gets absorbed, and participates in the reduction reaction $C(s) + CO_2 \rightarrow 2CO$. The CO thus formed is desorbed to diffuse away from the solid and to encounter the inward diffusing oxygen. The reaction between CO and O_2 gives a blue flame according to $CO + O_2 \rightarrow 2CO_2$. Part of the CO_2 thus formed returns to the surface to start the cycle again. Although the temperatures of both the solid surface and the CO flame are high, the global carbon consumption rate is so small that the CO flame is generally situated quite close to the solid surface except when the pressure and the oxygen content of the ambient gas are very low.

The temperature of charcoal and carbon surfaces is known to rise with an increase in the speed with which air is blown on them [9-12]. While the solid geometry, char grade, air temperature, and the size of the solid body are found to be of influence, more important is the fact that an increase in the air speed would increase the surface temperature. This behavior is in complete contrast with what is expected with gas phase flaming combustion wherein an increase in flow veloicty is known to increase thermal dilution as a consequence of which the flame temperature would fall to eventually result in an extinction of the flame.

In the case of heterogenous combustion, however, the very same mechanism by which thermal dilution is realized also brings about an enhanced oxygen diffusion to the reaction site at, or on, the surface. It is this enhanced

oxygen transport which is reponsible for the noted dependency of the reaction temperature on the flow velocity. This peculiarity is relevant to the blast/fire interaction as described in the following simple analysis.

Analysis:

Consider a glowing carbon surface. The oxygen mass fractions in the ambient air and at the reaction surface are respectively $Y_{O\infty}$ and Y_{Os}. Transfer of oxygen to the surface occurs as dependent upon the flow and geometry at a rate $\dot{W}_O'' = h_D(Y_{O\infty}-Y_{Os})$ where $\dot{W}_O''$ is the mass of O_2 transported per unit surface area per unit time and h_D is the mass transfer coefficient (kg/m^2s) obtainable for the given geometry as a function of the body size, diffusivity of oxygen, density of the gas phase, and the Reynolds and Schmidt numbers of the flow. If f is the stoichiometric fuel oxygen mass ratio, the carbon mass loss rate per unit area is

$$\dot{W}_s'' = f\, h_D(Y_{O\infty}-Y_{Os}) \tag{17}$$

If first order reaction kinetics are assumed, the chemical reaction rate is given by

$$\dot{W}_s'' = k_s Y_{Os} \tag{18}$$

where the specific reaction rate constant depends on temperature according to Arrhenius law.

$$k_s = k_{Os}\, \exp(-E_s/\bar{R}T) \tag{19}$$

where $E_s/\bar{R}$ is the activation temperature for the glowing reaction. Combining Eqs. (17) and (18),

$$Y_{Os} = Y_{O\infty}/[1+\frac{k_s}{fh_D}] \tag{20}$$

$$\dot{W}_s'' = Y_{O\infty}/[\frac{1}{k_s}+\frac{1}{fh_D}] \tag{21}$$

k_s/fh_D is a Damkohler number related to the surface glowing reaction. When this is very small, due to low pressures, temperatures or high mass transfer rates, the surface mass fraction of oxygen departs from the free stream value only

slightly. The oxgen mass gradients then are vanishingly small. The process is governed by the slow chemistry so that $\dot{W}_s'' = k_s Y_{O\infty}$. On the other hand, if the Damkohler number is extremely large since k_s is very large compared to the relatively sluggish mass transfer, $Y_{Os} \approx Y_{O\infty}/[k_s/fh_D] \approx 0$. Severe composition gradients arise and the situation is governed by the slower process of mass transfer so that $\dot{W}_s'' = fh_D Y_{O\infty}$.

An energy balance may now be derived by combining the energy and oxygen species conservation equations in the following form indicative of the correspondence between the depletion of O_2 and heating of the surface.

$$\frac{C_{pg}(T_s-T_\infty)}{h_c-C_{pg}T} = \frac{f(Y_{O\infty}-Y_{Os})}{(1+fY_{O\infty})} \tag{22}$$

Combining Eqs. (20) and (22), with Eq. (19),

$$P_s = \frac{(\theta_s-\theta_\infty)e^{1/\theta s}}{[(q_s-\theta_\infty)Y_\infty-(\theta_s-\theta_\infty)]} \tag{23}$$

where

$$\theta_s \equiv \bar{R}\,T_s/E \qquad \theta_\infty \equiv \bar{R}\,T_\infty/E$$

$$Y_\infty \equiv \frac{fY_{O\infty}}{1+f\,Y_{O\infty}} \qquad P_s \equiv \frac{k_{Os}}{fh_D} \qquad \text{and} \qquad q_s = \frac{\bar{R}h_c}{EC_{pg}}$$

This result is similar to Eq. (16) which corresponds to gas phase flaming. In Figure 10, Eq. (23) is depicted schematically. If the length of time the wood has been burning since its ignition is long, the char can be expected to be of high quality in its carbon content. Judging from the experimental data of Refs. 9-12, charcoal glowing temperature is lower than that of graphite. As a result, one can expect that graphite could be ignited to glow with lesser effort in providing oxygen, i.e., the Damkohler number for glowing ignition of graphite is higher than that for charcoal. Hence if the time of wood burning since ignition determines the quality of char, Eq. (23) for short and long burning times should appear as indicated in Fig. 10.

That an increase in air flow velocity (which causes a decrease in Damkohler number) will increase the glowing surface temperature is thus explainable. The main point is that the middle branch of the solution is forbidden only for the gas phase combustion; for glowing combustion it constitutes an allowable, although unstable, solution.

Blast/Charring Fuel Fire Interaction:

Consider the scenario, based on one first enunciated by Stan Martin [13], involving the following chain of events. A charring solid, such as wood, is ignited by a thermal pulse. The material burns with vigorous flames which progressivley become stronger as burning continues. The wood at the surface gradually transforms to char whose graphitic quality progressively increases as burning continues and pyrolysis penetrates into the solid. The air blast wave now arrives to strip, or blow, the flames away. The gas phase adjacent to the solid surface becomes rich in oxygen. The char surface ensues to glow and glow intensely if the blast winds are intense. This glowing provides a strong energy source which continuously supplies energy that is conducted into the solid to cause continued pyrolysis. As the winds subside, the glowing Damkohler number increases, the glowing surface temperature decreases to attain in time the frozen solution. As a result of the temperature decrease, the reaction would further diminish to reduce Damkohler number taking the system down along the frozen branch. In the course of this last excursion, if the system passes through the flaming ignition state, reignition (or reflash) of a flame would occur. If not, the fire just dies down.

This scenario is depicted in Fig. 11. The flaming combustion of a wood firebrand is indicated by the curve marked $OI_fE_fI_f'$ which is based on the same ideas as underlying Eq. (16). Flaming ignition occurs from state I_f to state I_f' to achieve a flame on the equilibrium branch. Branch I_fE_f is forbidden for the flame. As the firebrand undergoes flaming combustion in a thermochemical state near I'_F and as a blast wave is inpacted on its flames, the flame cools down towards the E_F state. If the blast is strong enough to cool the flame to E_F, flame extinguishment is imminent in the same way as if the flame is supported by a liquid fuel. There is one difference, however. Upon extinguishment of a liquid fuel flame, the state E'_F is attained. With charring fuel flame extinguishment, however, the corresponding post-extinction state is either E'_{F1} (for short preburn duration) or E'_{F2} (for long preburn duration)* on the charring unstable middle branch. Upon extinction of the flame to arrive at E'_{F1} or E'_{F2}, continued high winds may increase the glowing intensity to briefly drift the system E'_{F2} to A_2 or from E'_{F1} to A_1. The system will then cool down,

*By preburn duration, we mean, the time the wood has been burning before the blast arrived upon it.

as the winds subside, through the sequence of states A_2 -E'_{F2} -I_{G2} or A_1 -E'_{F1} -I_{G1}. Due to the corresponding reduction in the temperature of the reacting surface, the chemical kinetic rate itself would soon begin to fall from I_G to 0. In the course of this state transition, the system may encounter the flaming ignition point I_F if the preburn char is so as to correspond to $E_G E'_{F2} I_{G2}$; the flame would then reflash to I'_F when the preburn time is long. On the other hand, if the preburn time is short such as that corresponding to $E_G E'_{F1} I_{G1}$, the process of $I_{G1}0$ of cessation of the reaction would never pass through the flaming ignition state I_F and hence no reestablishment of the flame is possible.

If the effect of preburn time is not to alter the graphitic nature of the surface char but to modify the flammability properties of the pyrolysis gas mixture, the flame reflashing may be explained as shown in Fig. 12. Since a longer preburn may be expected to improve the quality of combustibility of the pyrolyzates, the curve $0I_{f2}E_{f2}I'_{f2}$ represents the long preburn flaming situation. Ignition of these pyrolyzates is easier and the equilibrium flame temperature is higher. Flaming of the products of pyrolysis resulting at earlier times (i.e., short preburn ime) is representable by the curve $0I_{f1}E_{f1}I'_{f1}$ wherein ignition is relatively difficult and the heat of combustion is relatively smaller. Experience on wood crib burning, however, leads one to believe that the preburn time may influence the quality of pyrolyzates only in a minor way.

The char glowing combustion, invariant with time of preburn, is indicated by curve labelled $0I_G E'_{f1} E_{f2} 'E_G$. Now focussing on the short preburn situation as a blast wave shifts the flame to E_{f1} extinction occurs to the char state E'_{f1}. As the winds subside, the char glowing rate decays from near E'_{f1} to I_G and the reaction dies from I_G to 0. In this last leg of state oxcursion from I_G to 0, the system does not encounter the flaming ignition state I_{f1}. Hence this short preburn situation involves no reflash of the flame.

Take the long preburn situation in the same sequence of arguments and one sees that as the flame is blown out, glowing is thwarted by the subsiding winds and the char is cooled down, the pyrolyzate flaming ignition state I_{f2} is surely encountered to result in a reflash of the flame to I'_{f2}. Thus as the preburn time increases, the pyrolyzates issued are more flammable, I_f shifts to the left from I_{f1} towards I_{f2}. There is a minimum preburn time beyond which the flaming ignition state I_f falls on, or to the left of, I_G which corresponds to the

conditions of flame reflashing.

Note that with the reflashing considerations, the ignition characteristics of the flammable gases as well as the char become relevant. This is unlike their relevance in Class B fire interaction with the blast.

EXPERIMENTS, CORRELATIONS AND DISCUSSION

SRI Experiments:

The most abundant and relevant experiments to test the blast/fire interaction hypotheses of the preceding chapter are those reported by Martin, Backovsky and their colleagues at SRI International [1-3]. The experimental set up and data will be briefly discussed in this chapter before adapting the data for correlations in the conceptual framework of ignition and extinction.

The properties of concern in the hypothesis may be conveniently placed into three categories respectively pertaining to the fuel, fire, and the blast. Among the fuel properties are: the pyrolysis kinetics of wood fuel or the vaporization thermodynamics of liquid fuels, thermodynamics of mixing, thermochemistry of glowing and flaming combustion, oxidation kinetics of glowing and flaming reactions, and transport properties. The fire properties mainly concern the geometry (shape, size, orientation) of the fuel bed, the nature of flow (forced or free convection) and the externally imposed radiant flux. The blast properties include the peak overpressure, time of positive phase and continued radiant pulse.

The SRI experimental facility attempts to capture these essential variables as described in detail by Martin and Backovsky in references 1-3. Suffice it here to say, the air-driven shocktube is capable of producing shockwaves typical of those produced by kilo-to-megaton nuclear explosions in air. The peak over pressures (up to 25 psi) and positive phase durations (between 0.10 to over 3.5 sec) are prescribable by the operator in this experimental set up. The test section and typical wood crib are shown in Figs. 13 and 14.

Liquid pool fires are tested with a variety of fuels: n-hexane, methanol, kerosene, n-pentane, and acetone with the fuel bed length ranging between 12 and 36 inches. The mean overpressure is varied between 0.91 and 7.5 psi. Time of positive phase duration was ranged between 0.068 and 3.8 sec. In some tests, the preburn time before the blast arrival is noted. Barriers located upstream of the pool are also studied in some tests. The observations included noting whether or not a given fire is extinguished by a given blast.

Typical wood cribs shown in Fig. 14 are made of (mostly) dry western hemlock and (some) redwood. Overpressures in the range 0.91 to 9.88 psi with

positive phases between 0.078-0.117 sec are tested. The cribs are made of sticks either 3/8" or 3/4" thick. A tray of propyl alcohol under the crib is used to prompt the crib ignition following which the crib is allowed to burn for anywhere from about 60 - 180 sec before the blast wave is imposed on the fire.

There are also reported eleven tests in which trays of shredded blotter or filter paper act as fuel beds.

Correlation:

We first acknowledge that it is always a precarious task to undertake interpretation of other investigators' experimental data. Only the experimentor knows all the subtle details of the set-up, conduct and behavior of an experimental run. However, opportunity exists to improve the current knowledge of blast/fire interaction by testing the hypothesis of this report. We take the SRI data at their face value as documented in references 1-3 and as understood in the sporatic discussions between the experimentors and the present author. Having made note of this limitation, we now seek to gather the information required to adapt the experimental data to the hypothesis of the preceeding chapter.

Class B Fires:

Our intent is to present the SRI data in the format of Fig. 9. In order to transform the coordinates into nondimensional form, the following details are to be noted.

$q \equiv \bar{R}\, h_c Y_{Ai}/E\, C_{pg}$. The universal gas constant requires no comment. Enthalpy of combustion for various liquid fuels is well known. The mass fraction at the fuel boundary Y_{Ai} depends on the pressure as well as temperature at the boundary. Prior to the blast arrival the surface concentration will correspond to equilibrium vaporization. Immediately following the blast arrival, the flame will be disturbed; there will be significant mixing. The rise in temperature due to shock compression will be too rapid for the condensed phase to promptly respond. We take here the fuel concentration to be same as that in stable equilibrium diffusional combustion. For most hydrocarbon fuel pools burning in air, the fuel concentration at the surface can be estimated to be about 1 kg/m^3. This quantity is obviously a function of the saturation vaporization process in which such parameters as the liquid temperature, latent heat of vaporization play

a role. The precise delineation requires a fundamental study of liquid vaporization, such a study being out of the scope of the current project. The quantity Y_{Ai} thus would be taken as $1(kg/m^3)/\rho(kg/m^3)$ where ρ is the air density at a pressure representative of the conditions immediately following the blast arrival. The specific heat of gases will be taken to be a constant equal to 1666 J/kgK irrespective of the temperature and composition. This again is an approximation without which the application becomes horrendous. Literature [7] on combustion of hydrocarbons in air indicates that the global activation energy E ranges between about 150 to 250 MJ/kgmole depending upon the fuel an the combustion situation. In studies not seeking to elicit the actual elementary chemical reaction steps culminating in the global behavior, it is fairly safe to take E to be approximately 200 MJ/kgmole, independent of the hydrocarbron. One thus estimates q as

$$q \approx 2.8\times10^{-7}\ h_c(\text{in J/kg})/P(\text{in psia}) \qquad (24)$$

The units are inelegantly mixed because h_c is generally known in SI units and the experimental tabulations give pressure in psi.

$P = k_0\ell/u$. We take the velocity u to be the particle velocity produced by the blast. By the relation given on page 6, with $\gamma = 1.4$ for air whose pressure prior to shock arrival is $P_0 = 14.7$ psia, and speed of sound in ambient air $c_0 = 1076$ ft/s, we find $u(\text{in ft/sec}) = 1076\ \rho/[20.58\text{x}(1+0.0583p)^{1/2}]$ where p is the peak overpressure in psi. Furthermore, the global collision frequency k_0 of the assumed first order oxidation reaction is taken to be $5\text{x}10^{10}(1/\text{sec})$ independent of the fuel within the same restraints of approximation as the global activation energy discussed above. One would thus obtain

$$P \approx 1.5\times10^{9}(1+0.0583\ p\ (\text{in psi})^{1/2}\ \ell(\text{in inches})/p\ (\text{in psi}) \qquad (25)$$

again the units being written for the convenience of adoption to experimental data. ℓ is the fuel bed length.

Tables 1-4 are directly taken from references 1-3 to report the class B fire data involving no barriers. Forty six different tests are involved in these tables on five different fuels with three tray lengths. The blast strength parameter P and fire strength parameter q are estimated for each run according to the preceding explanation and columns are added to the original tables. The data are shown plotted in Fig. 15 in coordinates suggested by our hypothesis of

Fig. 9 delineating the regimes in which the flame would be extinguished from those in which it would sustain the blast. The closed symbols correspond to flames which are extinguished while the open ones stand for flames which resisted extinction.

The boundary curve shown in Fig. 15 is precisely the same as the one in Fig. 9 except that it is shifted upwards by a factor of 10^9. This is permissible since our entire theoretical effort is not meant to be a development of a prediction capability. Instead its goal is to develop concepts and general forms of the nondimensional descriptions of the paramters. Thus shifting the curve of Fig. 9 so that it passes through $q = 0.55$ and $P = 25$, the boundary between the extinction domain and nonextinction domains is obtained.

With the exception of the four anomalous experiments in which extinction occurred when it is not expected*, the hypothesis bears well in separating the conditions suitable for extinction from those unsuitable. In fact the goodness of this separation is especially impressive if one recalls that the hypothesis is based on a theoretical model of remarkable simplicity.

The global combustion chemistry kinetics are not well-known. Transport properties are poorly defined. The mixing, cooling, and dilution following the arrival of the blast wave is certain to be hopelessly complicated for any level of theoretical description. There will undoubtedly be alterations in the vaporization thermodynamics as the blast effects of imposed. The surface fuel vapor concentration assumption is admittedly an over-simplification. Not withstanding all the rough spots in the evolution of the theoretical hypothesis underlying the map of Figs. 9 and 15, the success is indeed gratifying.

Attention is drawn to the fact that, in preparing Fig. 15, the length of positive phase duration is not at all invoked. That even this omission did not influence the validity of the hypothesis underlying Fig. 9 indicates that if the fire did not get seriously disturbed towards extinction in the very first few milliseconds of blast impact, it most probably is going to survive the blast. This is an interesting inference, for it suggests that the future predictive theories may perhaps be based on a description of the events promrtly surrounding the very initial stages of the blast/fire interaction.

The SRI data also include some runs in which a 1.75" barricade wall is placed upstream of the fire. Although theoretical solution of the problem

*These anomalous runs are run #7 of Table 1 on hexane, run #2 of Table 3 on kerosene and runs #8 and 10 of Table 3 on pentane.

describing the influence of barricades on blast/fire interaction requires detailed analysis and calculations, one can expect barricades to generally stabilize fires. As the flow occurs over a barricade step, strong recirculation of flow is expected behind it. Such a recirculation will in effect slow the flow down (or increase the flow path length and flow time). The net result is that the presence of a barricade will increase the nonextinction domain of the P-q map by displacing the boundary curve downwards.

The SRI barricaded pool fire data from Reference 2 is reported in Tables 5 and 6 with columns added for P and q. The data are plotted in Fig. 16. Except for the anomalous run #64 of Table 6 on hexane, the downward shift of the boundary curve is evident both for hexane and methanol fires. Note, however that the height of barricades tested (1.75") is relatively small compared to the length of even the shortest fuel bed. Such short barricades at best are expected to modify the flow profiles without producing significant stable recirculation. Experiments in which the barricade height is comparable in magnitude to the pool length appear to be desirable to simulate the influence of a window-sill in the interaction of a blast with a fire in a room. No systematic extinction-nonextinction boundary curves can now be drawn on the basis of the available short barricade data presented in Fig. 16.

In Reference 3 Backovsky draws the conclusion, based on high-speed photographic observations, that the most plausible mechanism of class B fire extinction by blast is one based on displacement of the flame from the fuel surface. This is not inconsistent with the hypothesis of this report in which the definition of extinction evolved to be an annilhilation of the flame by whatever specific details. Excessive cooling and dilution to levels prohibiting flame reflashing from downstream is within the realm of our hypothesis. Through the success apparent in Figs. 15 and 16, it is fair to say that expectable trends of extinction behavior are achieved as dependent upon the fuel type, pool size, and blast strength, with as well as without the barricades.

Class A Fires:

The SRI experiments on blast interaction with wood crib fires indicate that the length of time a crib is permitted to burn before the blast imposition (i.e., the 'preburn time') has a strong effect on the extinction process. Cribs with longer preburn time require stronger blasts for extinction. Even more interestingly, the experiments show that if the preburn time exceeds a certain

minimum value (≈170s corresponding to a minimum fractional weight loss ≈ 35%), the fire sustains the impact of any blast (in the tested 1-10 psi overpressure range) irrespective of the blast strength.

In attempts to represent the blast/fire interaction for class A fires on the same basis as class B fires presented above, several questions arise. These questions mainly pertain to the pyrolysis of wood and wood-like solids as they burn in the format of a crib. Specifically how does the preburn time make the fire progressively stronger and eventually strong enough to become immune to extinction? Said another way, how does one nondimensionlize the preburn time to obtain a parameter which is capable of serving as a measure of the fire's energetic strength? One can surmise that continued heating of wood will gradually enhance the combustibility quality of the pyrolyzates. But this speculation is dismissed by the observation that the crib burning rate attains a steady maximum value in a reasonably short time. Indeed, it appears that no argument based on gas phase combustion phenomena yields a viable basis to explain the SRI experimental trends.

Therefore, we turn to the solid phase phenomena of transient conduction and pyrolysis. As crib burning continues during the preburn time, the solid is continuously heated up due to conduction. Also the pyrolysis process develops within the solid transiently to evolve into an inward propagating wave. Our following treatment is based on the premise that the transient heating process improves the blast resistance of a crib fire as progressively more energy is stored within the fuel element to sustain a certain inertia to the pyrolysis and combustion process. An appropriate time scale for this effect appears to be the burning time constant t^0 which represents the time taken by a fuel element to completely char. The nature of t^0 is discussed in later paragraphs.

If the ratio of preburn time to the burning time constant represents the gradually increasing blast resistance of the crib fire by the above argument, what factors determine the critical preburn time beyond which the fire becomes blast-proof? The answer to this question is sought under the premise that at this critical time, the surface of the fuel element is completely charred so that at times longer than this the pyrolosis wave is fully developed to propagate into the solid thus gradually increasing the thickness of the surface char layer. Based on pyrolysis kinetic data, the critical preburn time can be estimated.

Burning Time Constant t^0:

Backovsky et al [2,3] give an excellent summary of the state-of-the-art knowledge about the burning behavior of wood cribs. Most notable in this summary are the facts that: (a) the crib burning quickly attains a steady state in which more than the middle 50% of the total mass loss would occur such that mass decreases linearly with time; (b) this steady state burning rate depends upon both the stick thickness and the packing density of the crib; (c) for loosely packed cribs the steady burning rate is given by $\dot{m} = K A_s/\sqrt{b}$ where $\dot{m}$ is the rate, A_s is the total surface area of the exposed wood in the crib and b is the stick thickness. The constant K depdnds upon the type and moisture content of the wood. $K \approx 1.05 \times 10^{-3}$ gm/cm$^{1.5}$ sec for pine cribs with moisture content in the range 5-10%; and (d) the feedback from the flame in the plume over the crib (i.e., 'topflame') is not a significant factor in determining the steady rate of crib burning.

The square-root dependence of burning rate on stick thickness is empirical. Kanury [14] theoretically deduced the time to completely char a cylindrical wood element under well-ventilated crib conditions as

$$t^0 = A\, b + B\, b^2$$

where b is the element thickness and A and B are constants defined as below.

$$A \equiv [L(\rho_0-\rho_c) + \rho_0 C_{p0}(T_p'-T_0)/2]/2\dot{q}''$$

$$B \equiv 1/(32\, \alpha_0)$$

where L is the latent heat of pyrolysis of wood ($\approx$ 300 J/g volatile production), ρ_0 is original wood density ($\approx$ 0.6 g/cm^3), ρ_c is final char density ($\approx$ 0.15 g/cm^3), C_{p0} is original wood specific heat ($\approx$ 2J/g K), T_p' is temperature at which wood pyrolysis is significant ($\approx$ 600 K), T_0 is initial temperature ($\approx$ 300 K), α_0 is the wood thermal diffusivity ($\approx 1 \times 10^{-3}$ cm^2/s) and $\dot{q}''$ is the heat flux involved in the mutual interaction among elements within the crib ($\approx$ 0.5-2.0 J/cm^{2}s). Noting that t^0 is related to steady burning rate $\dot{m}$ through the crib initial mass m_0 according to $t^0 \approx m_0/\dot{m}$. The empirical relation highlighted by Backovsky leads to

$t^0 \propto b^{1.5}$. However, our theoretical relation indicates that while thin fuel elements have a burning time t^0 proportional to b, thick elements are consumed as $t^0 \propto b^2$. While the heat flux and pyrolysis energetics (and kinetics) play a dominant role in thin element pyrolysis, transient conduction within the solid predominantly governs the thick element pyrolysis. The effect of moisture in the solid can be taken into account by increasing the heat of pyrolysis L.

For reasonably dry wood then, taking $\dot{q}''$ to be 0.6 J/cm^{2}s,

$$t^0 \approx 262\ b + 31\ b^2$$

where t^0 is in seconds and b is in centimeters. The fire strength q then is proportional to the ratio of preburn time to t^0. A plot of the blast strength paramter P against this ratio is expected to differentiate conditions of crib flame extinguishment from those of nonextinguishment. By the experience obtained from Figures 16 and 17, since the boundary curve appears to be same for different fuels and since the wood pyrolyzates are mostly a mixture of several hydrocarbons and carbohydrates, there is reason to believe that the boundary curve for wood flame extinction is approximately same as that for class B fires. As a result, q for charring fuel fires is denoted by τ and defined as $\tau \equiv 2.7$x preburn time/t^0. The factor 2.7 is obtained from trial and error to account for possible differences between class A and class B fires. A justification for this is yet to be developed.

Surface Charring Kinetic Time:

Wood pyrolysis is generally known to be an extremely complex chemical kinetic process. However, it is customary in most theoretical analyses to take the pyrolysis process to be of order unity with the preexponential factor and activation energy respectively in the ranges 10^6-10^{19} 1/s and 100-200 kJ/gmole. Taking them to be 10^{10} 1/s and 140 kJ/ gmole, we can estimate the time taken by the surface to completely pyrolyze to be about 1.6×10^5 s at T = 500 K, 464 s at 600 K, 7.2 s at 700 K. The surface temperature of transiently heated wood rises nearly as the square root of heating time. Pyrolysis experiments reported by Kanury [15] indicate that the surface takes about 2 to 3 minutes of exposure to completely transform to char in a fire situation. Thus, the above estimation leads to a surface temperature of burning wood to be about 620 K at which the time to completely pyrolyze is about 170 s.

The critical preburn time beyond which the crib fire becomes blast-proof is noted in the SRI experiments to be also of the order of 170 s. Thus there seems to be reason to believe that this critical preburn time corresponds to the complete charring of the wood surface. Upon producing a char sheath with preburning longer than this critical time, the pyrolysis process is confined to the interior of the solid to become relatively insensitive to the blast effects in its immediate response. Additionally, the surface char has then become a more effectively glowing fuel to respond to the blast effects immediately in producing conditions of flame reflashing by the hypothesis postulated earlier. One would thus expect the flaming boundary curve to be transformed to a vertical line abruptly at τ = 2.7x critical preburn time/t^0. Since both the critical preburn time and t^0 depend upon the crib stick thickness, this critical τ may depend upon the stick thickness. Critical τ is estimated to be 0.85 and 0.65 respectively for 3/8 inch and 3/4 inch stick cribs. However, since scaling should alleviate this dependency on stick thickness and since the relation between q and τ is yet to be justified by a reasoned hypothesis, we take the critical τ to be 0.75, average of the values for the two thicknesses. Even if tentatively, this critical τ is presumed to be independent of stick thickness.

Tables 7-10 are directly taken from References 2 and 3 to report class A fire data with columns added for the blast strenth parameter P and the fire strength parameter τ. Thirty nine tests with 3/4-inch stick cribs, thirty four tests with 3/8-inch sticks and ten tests with trays of shredded paper are involved in this series. Three 3/4-inch redwood stick cribs are also tested and data given in Table 4. In nine of these 86 tests flame reflashing is noticed as the blast subsides. Although glowing of different intensities is observed in over a dozen tests, not all glowing tests experienced the flame reflashing. In some tests, the crib is noted to have burned poorly. In some others, the shock tube diaphragm ruptures poorly. In yet others, the reflashing occured as the test section is opened up to remove the extinguished crib from the tube. In two of the shredded paper tray tests, reflashing is found to occur when air is fanned over the glowing/smoldering fuel bed.

Suffice it to note, unlike class B fires, the crib fire experiments are extremely difficult to control. Although a great deal of care is excercised by the SRI team in the conduct of these experiments and although much valuable information is developed, there persist numerous ambiguities some of which may be impossible to be ever resolved. Keeping this in mind, the data of Tables 7-10 are shown plotted in Fig. 17.

Although the correlation of Fig. 17 appears to be less clear cut than the Class B fire correlations of Figs. 15 and 16, the success of the hypothesis is evident. All the shredded paper tray fires, one 3/4-inch redwood crib fire, and eight 3/8-inch hemlock stick crib fires defy the hypothesis of this report by failing to resist the blast extinction. Similarly, ten (3/4-inch hemlock crib) tests fail to extinguish where they are expected to. The most probably reason underlying these delinquent nonextinctions is that the thicker sticks in the crib provide more effective recirculation pockets conducive for stabilizing the flames. Nonetheless, it can be seen that the extinctions lie mostly within the extinction envelope and the nonextinctions, without it. Most of the reflashing is noticed at τ larger than 0.75 which may be recalled to correspond to complete charring of the solid surface. Almost all of these reflashed tests involve 3/8-inch stick cribs.

The shredded paper experiments seem in their majority to defy the hypothesis of this report. This behavior is perhaps understandable on the basis that smoldering of the shredded fuel bed is in many respects different from the burning of well-ventilated (loosley packed) stick cribs. Furthermore, the mechanical integrity of the shredded fuel beds is expected to be so poor as to enhance the cooling of the fuel elements by the blast winds. Flame holding recirculation zones are also minimal in these beds. Based on such factors, it appears reasonable to expect shredded fuel beds to be more susceptible to extinction by blast.

No particular pattern is discernible from the present correlation as to the reflashing mechanism. Thus the hypothesis postulated earlier can not be systematically tested at present.

CONCLUSIONS AND RECOMMENDATIONS

The Damkohler number P and the fire strength parameter q appear to constitute the major parameters in describing the mechanism of 'blowing-away' of flames due to the impact of a blast wave. While the Damkohler number represents inverse of blast stength, the fire strength parameter represents mainly the heat of combustion. Based on an algebraic model, a concept is developed to identify a map of P versus q on which the domain of conditions conducive to fire extinction can be separated from conditions unconducive. The hypothesis is tested by the SRI shocktube experimental data on a variety of class B and class A fires. Flames, on both liquid and solid fuels, appear to be blown out by the same mechanism. As shown in Figs. 15 and 17, the P required to achieve extinction is lower for flames of higher q.

The influence of an upstream barricade is shown to render the liquid fuel flames more blast-resistant so that the nonextinction region of the P(q) map is increased. No distinct boundaries, however, can be drawn now for the barricade effect. Experiments are required in which taller barricades are systematically tested. Theory describing the mechanism of flame stabilization by recirculation has to be developed to compare with these experiments.

The enthalpy of combustion of the fuel, fuel bed length, barricades and shock wave strength are the most important variables in the blast/class B fire interaction process. The fuel vaporization thermodynamics, including enthalpy of vaporization, the nature of wick holding the fuel in the pool, and combustion kinetic parameters appear to have little or no effect on the response of class B fires to blasts. This is a significant point since such properties as those pertaining to global oxidation kinetics can not be expected ever to be known in reliable and quantitative detail.

The hypothesis of blast/fire interaction postulated and tested with pool fire data in this report is capable of describing fire extinguishment viewed in different ways. For instance, if extinguishment is defined as annihilation of the flame, it includes both the degeneration of a stationary flame and 'nonreappearance' of a displaced flame. The flame displacement mechanism advocated by the SRI group thus is completely consistent with the present hypothesis. The success evident in the correlations of Fig. 15 is probably the proof of this consistency.

Having correlated the 12 to 36 inch long liquid pool fires, we believe the next task in studying class B fires is to develop ways of scaling the fires up to

several tens or hundreds of feet in size. Development of these scaling rules requires consideration of such additional factors as: thermal radiation feed-back from the larger flames to the fuel surface, effect of the size of the flames on the uniformity with which the blast would perturb them, accentuation of the recirculation phenomena, and others. Based on the definition of P , the critical fuel bed length is nearly proportional to the peak overpressure and the particle velocity. (See Eq. (25)). This conclusion is similar to that reached earlier by Backovsky et al in Ref. 2.

Turning now to class A fires as represented by cribs of wood sticks, we note that the mechanism of flame extinction appears to be the same as that of class B fires. The extinguished state, however, involves charcoal embers capable of undergoing a metastable glowing combustion process. This glowing combustion process supplies sufficient energy to the solid to continue production of pyrolyzates. As the blast effects subside, the cooling (and yet pyrolyzing) embers may pass through a thermochemical state corresponding to reflashing of flame in the pyrolyzate and air mixture.

Based on the knowledge of the composition of pyrolysis products, and of the relative independance of the extinction boundary of class B fires on the specific nature of the fuel, there seems to be no compelling reason to believe that the flame extinction boundary for crib fires will be different from that for class B fires. The correlation of P versus q to confirm this idea is given in Fig. 17. This correlation is not as clear-cut as that of liquid fuel flames.

The reasons for this can be any combination of such complications as following. (a) Although it appears logical to expect the preburn time to be an indirect measure of the fire strength q, the exact connection is not clear at present. Further study is required of this issue to establish the role of transient conduction (with pyrolysis) in rendering persistence and strength to a crib fire. (b) In a crib, opportunity exists for the flames to find intense recirculation zones behind individual sticks. These recirculation zones are more effective if the sticks are thicker. Because recirculation tends to stablize the flames and thus to shift the extinction boundary downwards, it is reasonable to expect nonextinctions where extinction would be expected in the absence of recirculation. That this is correct is visible in Fig. 17, especially in association with the (3/4 inch) thick stick fires. The future study recommended above, of flame stablization by recirculation, will aid in understanding the

effect of stick thickness on extinction. The high surface temperature of the wood sticks in a crib will be an important additional parameter to be considered in this connection. (c) The surfaces at different locations in the crib would char nonuniformly in all crib fires. The distribution of glowing patches which may expediently pilot the reignition of blown-out flames is thus a serious ambiguity of all crib fires. Resolution of this ambiguity requires further work. (d) Compared to liquid pools, the crib fuel beds are volumetric by two different counts, first by the crib structure itself and second by the conduction-controlled interior of the individual sticks. While the flames over pools are all-important in determining the pool burning rate, the flame over the crib (i.e., the 'top-flame') is of little or no significance compared to the flames within the crib. (e) Thermal radiation from the flames to the fuel surface is more or less unimportant in the class B fires in the size range tested. In contrast, thermal radiation plays a dominant role in the life, strength and death of a crib fire. Additionaly study is required to gain a better understanding of this role.

The data correlations of Fig. 17 also point out the possibility that the basic burning process of shredded paper fuel beds may be altogether different from that of cribs. It may be closer to that of liquid fuels, but this is yet to be examined by additional study.

The flame reflashing mechanism postulated in this report can not at present be tested by a correlation of the sort shown in Fig. 17. It is surprising, however, to note how few experiments in the SRI collection in fact show a distinct reflashing. In as much of charcoal glowing is expected to play an important role in this reflashing process, it appears important that a detailed study be undertaken of the effect of blast on glowing wood surfaces. The nature of glowing as it is distrubed by the blast variables, the implications in continued pyrolysis, and possible transition of glowing to flaming, are not only important in understanding the reflashing process but also exciting from the view-point of science.

Turning to scaling, not withstanding the complicated nature of wood crib fire burning discussed above, crib fires are probably easier to be scaled up since their burning is more or less locally controlled. Oxygen depletion in the depths of the crib may, however, become a crucial factor in such scaling endeavors. Thermal radiation effects, of course, are critically required. One important conclusion of the present study is that wood crib burning with and without blast interaction requires much further study before results useful in efforts of mitigation can be obtained.

REFERENCES

1. Martin, S.B., "Experiments on Extinction of Fires by Airblast," Annual Report, Contract DCPA01-79-C-0245, FEMA WU 2564A, SRI International, Menlo Park, CA (January 1980).
2. Backovsky, J., Martin, S., and McKee, R., "Blast Effects on Fires, "Annual Report, Contract DCPA01-79-C-0245, FEMA WU 2564A, SRI International, Menlo Park, CA (December 1980).
3. Backovsky, J., Martin, S.B., and McKee, R., "Experimental Extinguishment of Fire by Blast," Final Report, Contract EMW-C-0559, FEMA WU 2564A, SRI International, Menlo Park, CA (March 1982).
4. Glasstone, S., and Dolan, P., The Effects of Nuclear Weapons, U.S. Departments of Defense and Energy, USGPO stock No. 008-046-00093-0, (1977).
5. Rockett, J.A., "Outline of Fire Development Models and Their Status," pp. D-1 to D-4, Proceedings of Blast/Fire Interactions, Asilomar 1979 Conference. R.S. Alger, S.B. Martin, Editors, SRI International Report for DCPA, Contract No. DCPA01-78-C-0279, Work Unit 2563F (September 1979).
6. Carrier, G., Fendell, F., Feldman P., and Fink, S., "Forced Convection Extinction of a Diffusion Flame Sustained by a Charring Body," Final Report, Contract EMW-C-0371, FEMA, WU 2563G, TRW Defense and Space Systems Group, Redondo Beach, CA (May 1981).
7. Kanury, A.M., Introduction to Combustion Phenomena, Gordon and Breach Science Publishers, New York, NY (1975).
8. Williams, F.A., Combustion Theory, Addison Wesley, Reading, Mass. (1965).
9. Bhagat, P.M., "Wood Charcoal Combustion and the Effects of Water Application," pp. 275-291, Combustion and Flame, 37, (1980).
10. Kuchta, J.M., Kant, A., and Damon, G.H., Industrial and Engineering Chemistry, 44, pp. 1559-1563, (1952) as discussed in Appendix P of Combustion of Pulverized Coal by M.A. Field, et al, Published by the British Coal Utilisation Research Board, Leatherhead, England, (1967).
11. Smith, D.F., and Gudmundsen, A., Industrial and Engineering Chemistry, 23, pp. 277-285, (1934) as discussed in Appendix P of Combustion of Pulverized Coal.
12. Parker, A.S., and Hottell, H.C., "Combustion Rate of Carbon," pp. 1334-1341, Industrial and Engineering Chemistry, 28(11), (November 1936).
13. Martin, S.B., Personal Communication, (1982)

14. Kanury, A.M., "Rate of charring Combustion in a Fire," pp. 1131-1142, Fourteenth Symposium (International) on Combustion, The Combustion Institute, Pittsburgh, PA (1973).

15. Kanury, A.M., "Thermal Decomposition Kinetics of Wood Pyrolysis," pp. 75-83, Combustion and Flame, 18, (1972).

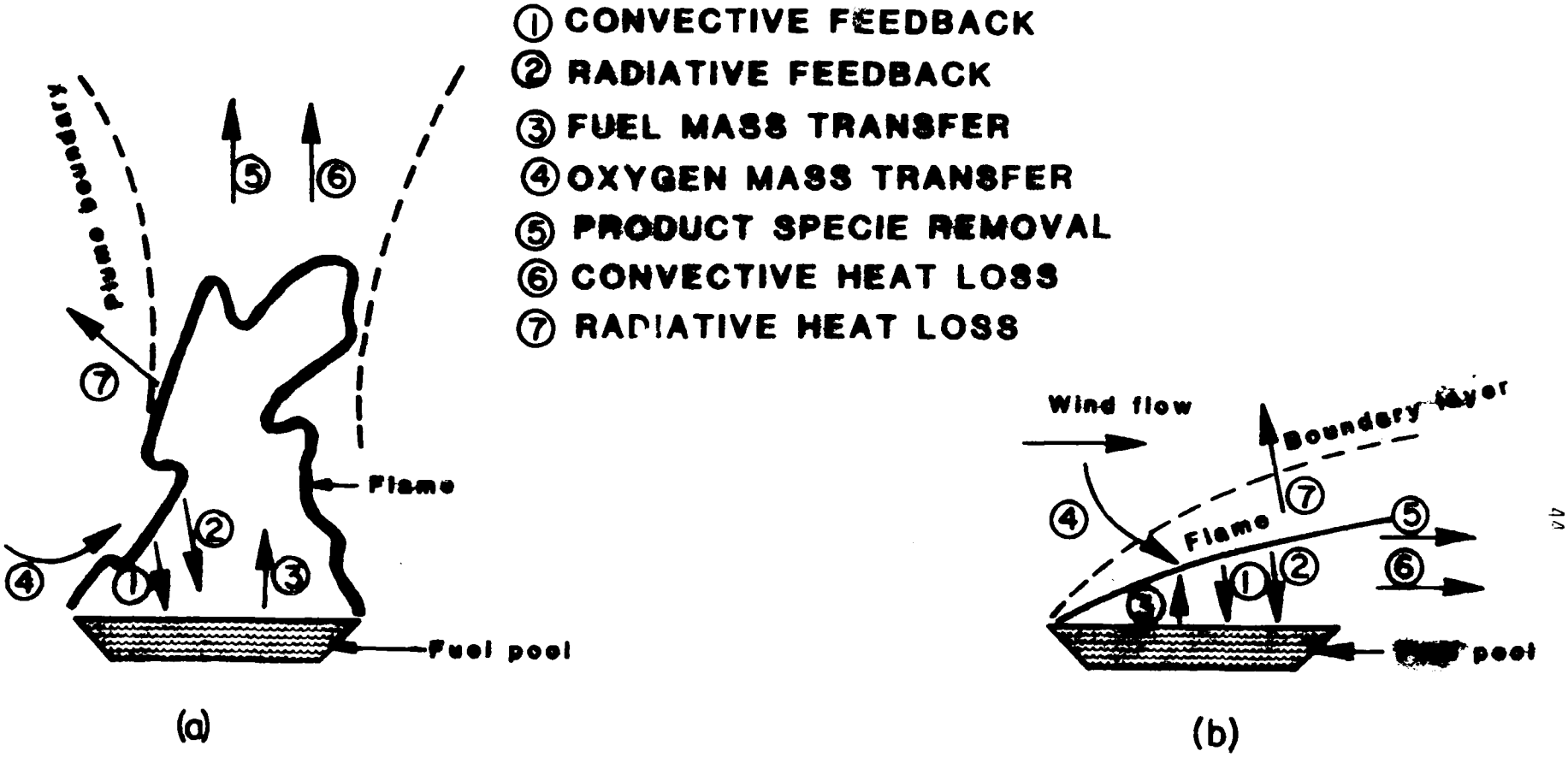

Figure 1. A Pool Fire (a) in Quiescent Air and (b) in a Wind.

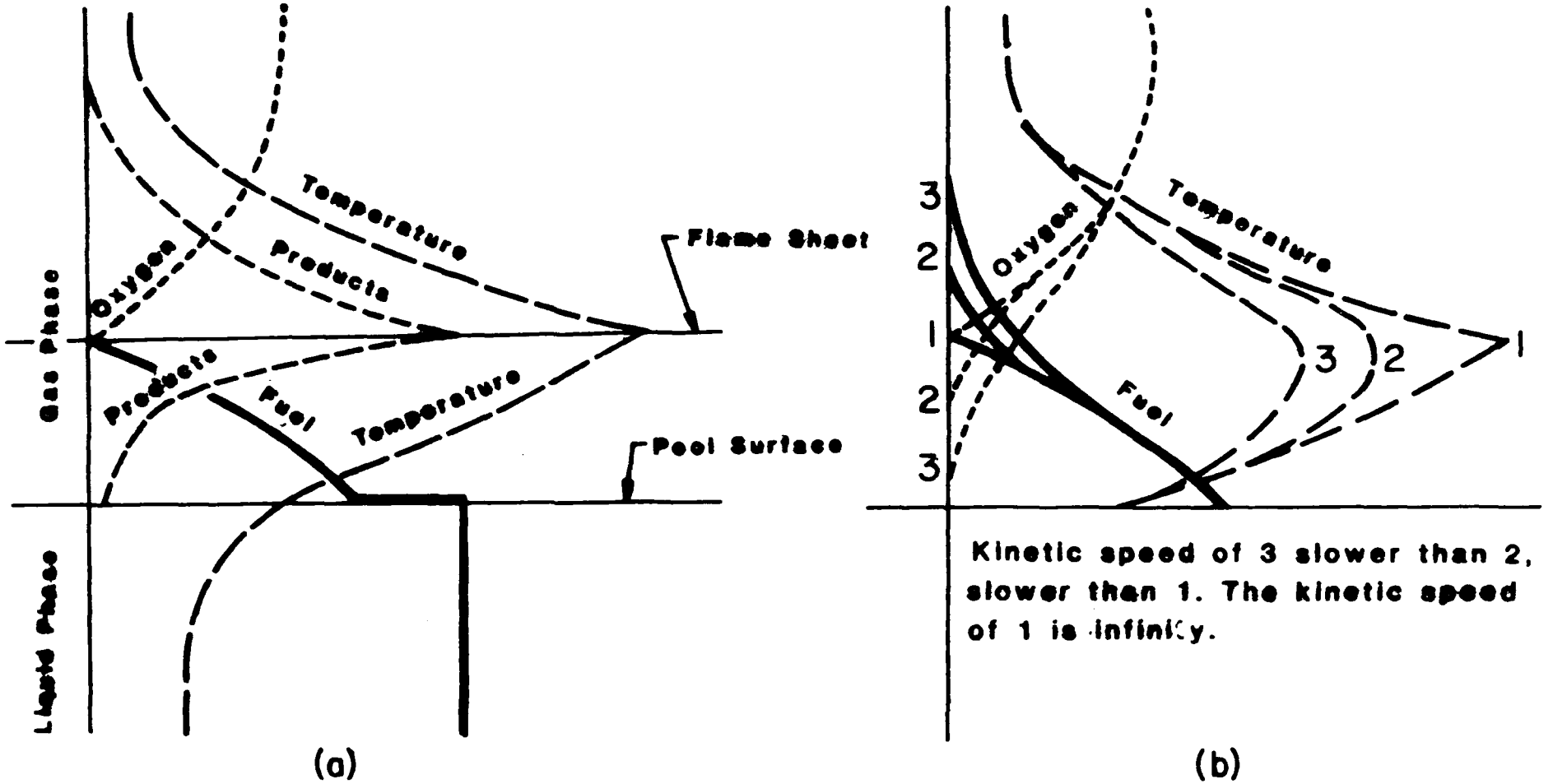

Figure 2. Flame Structure. (a) Ideal 'Diffusion flame'. (b) Effect of Finite Rate Chemical Kinetics.

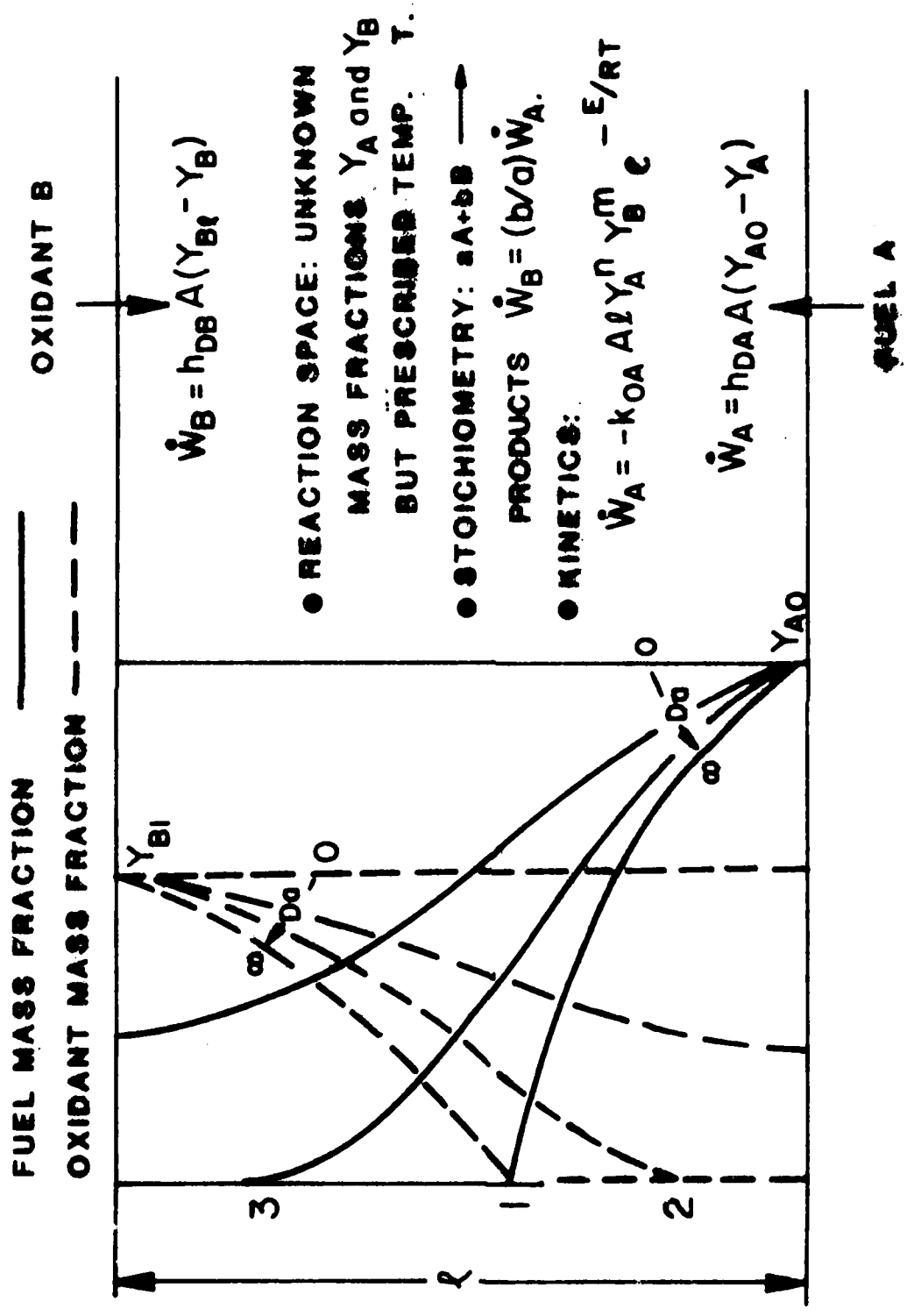

Figure 3. Effect of Damkohler Number on Species Distribution in a Reaction Space.

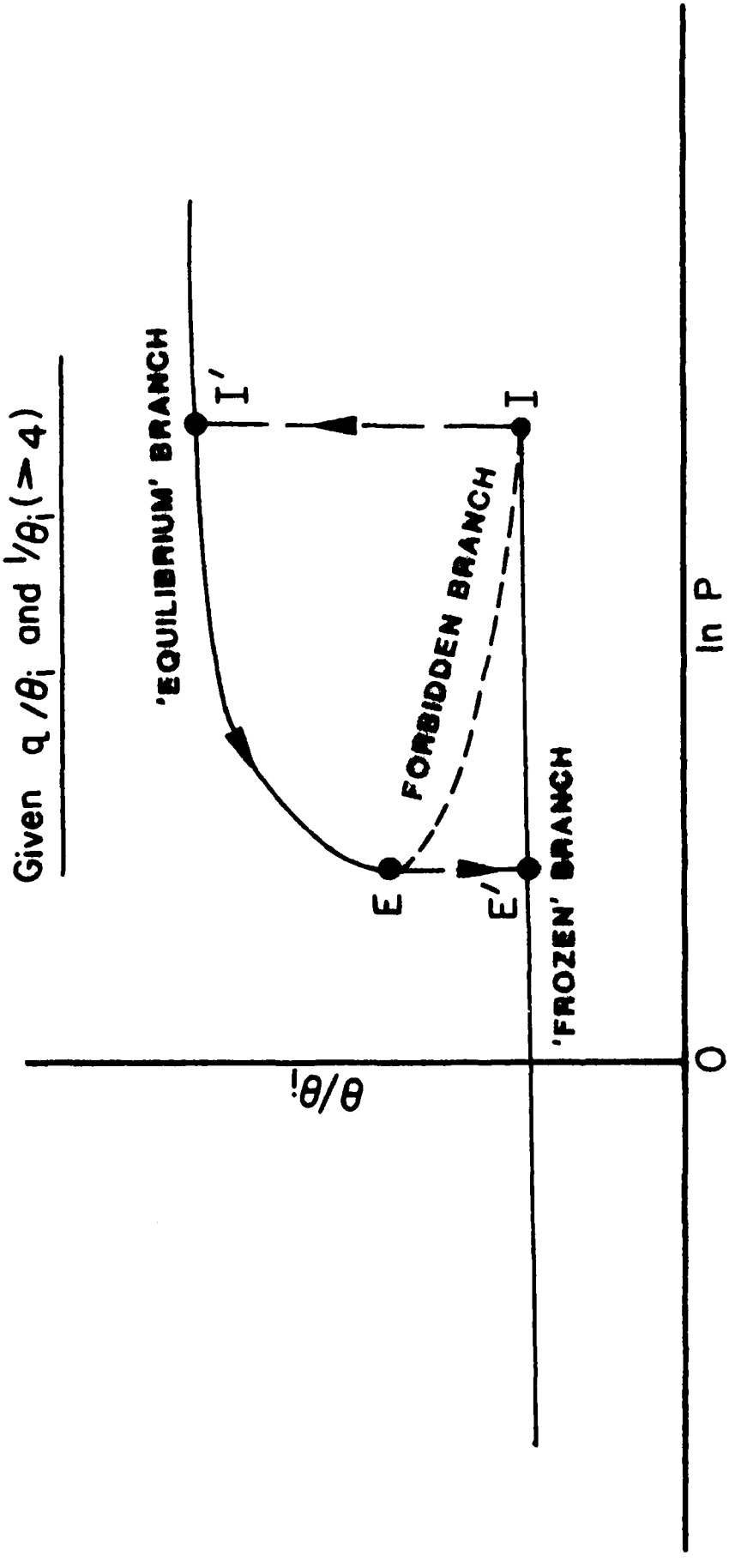

Figure 4. Reaction Temperature Dependence on Damkohler Number.

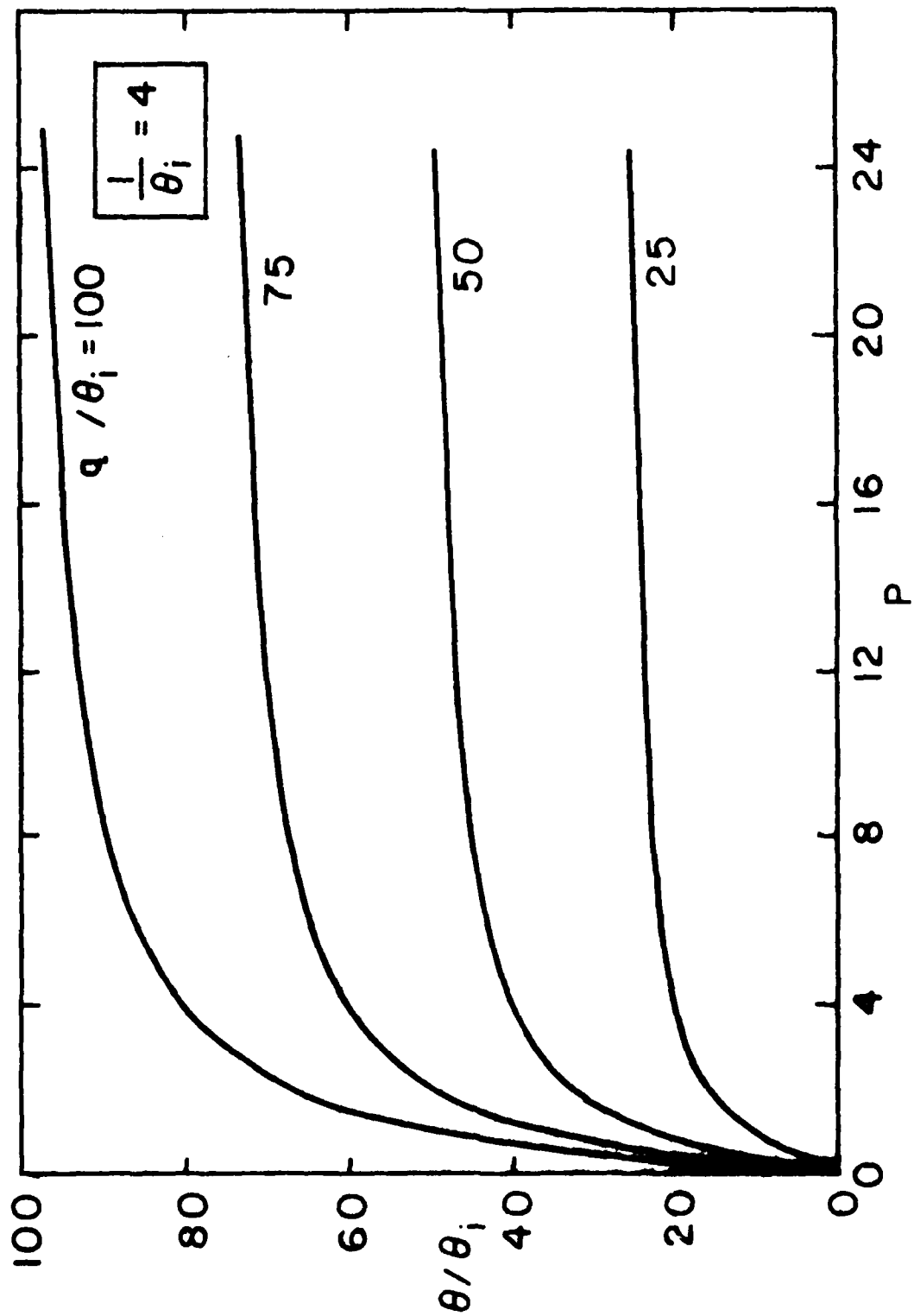

Figure 5. Reaction Temperature Dependence on Damkohler Number When Activation Energy is Low.

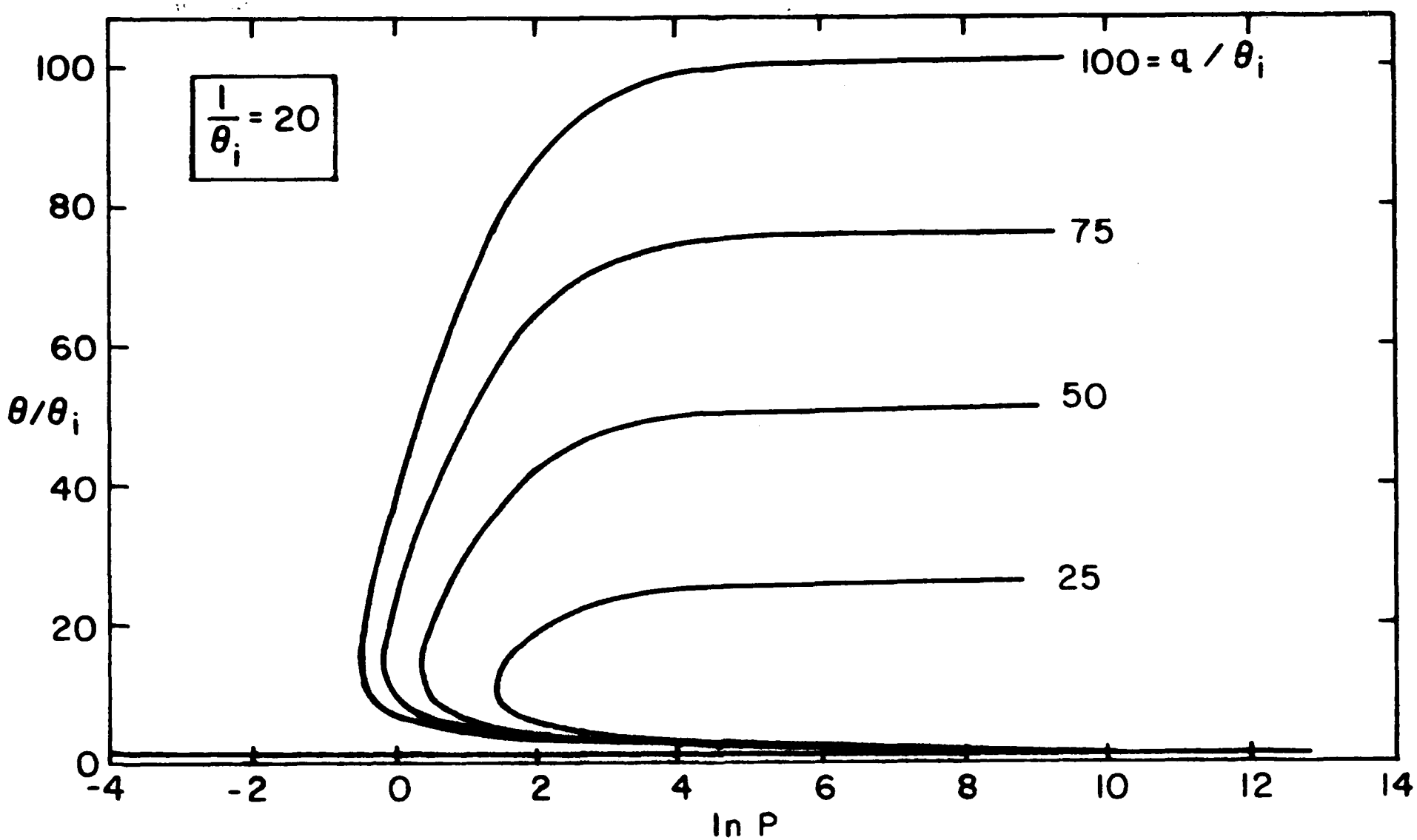

Figure 6. Reaction Temperature Dependence on Damkohler Number When Activation Energy is Moderate.

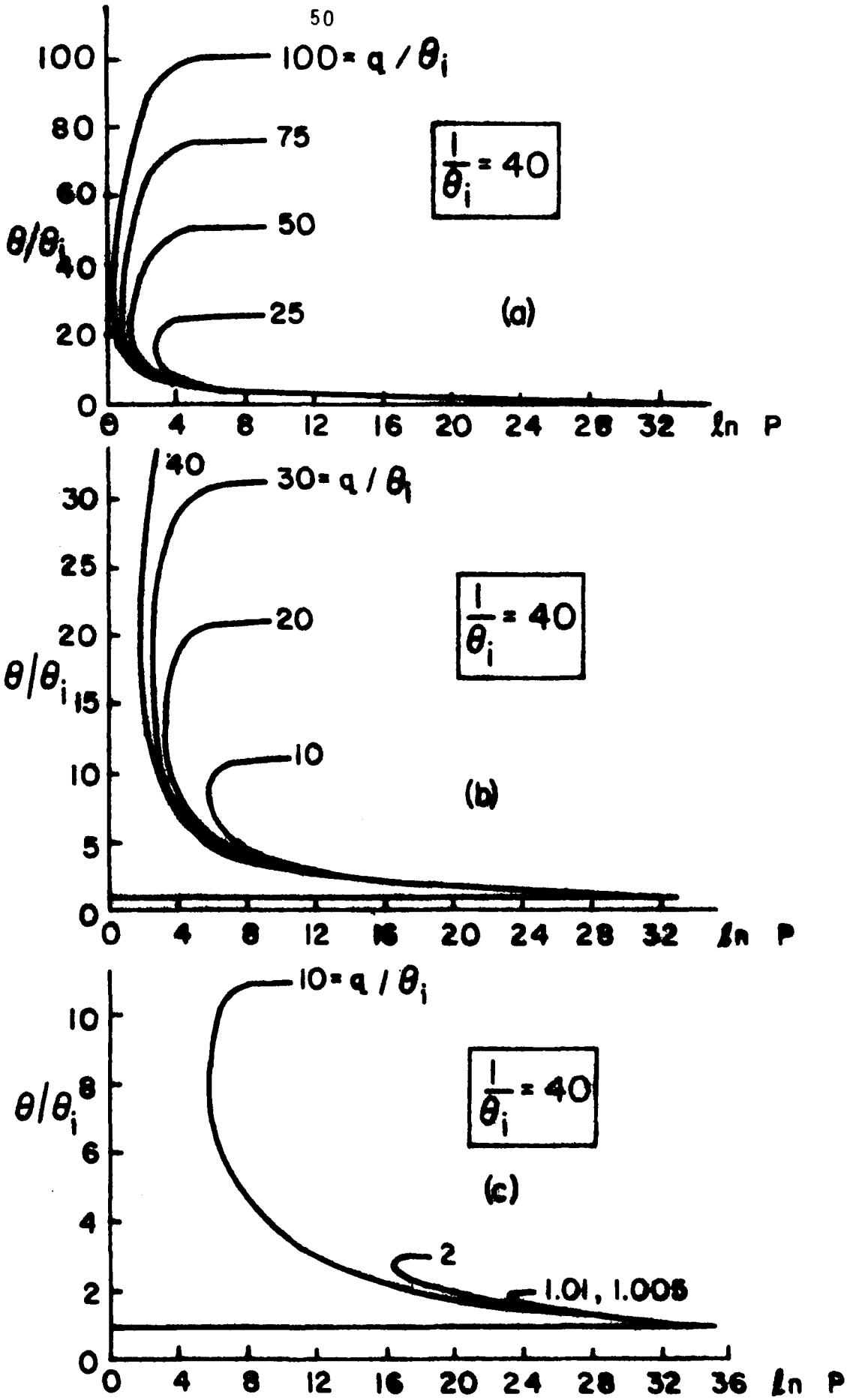

Figure 7. Reaction Temperature Dependence on Damkohler Number at Medium Activation Energy. (a) Large q ; (b) Medium q ; and (c) small q .

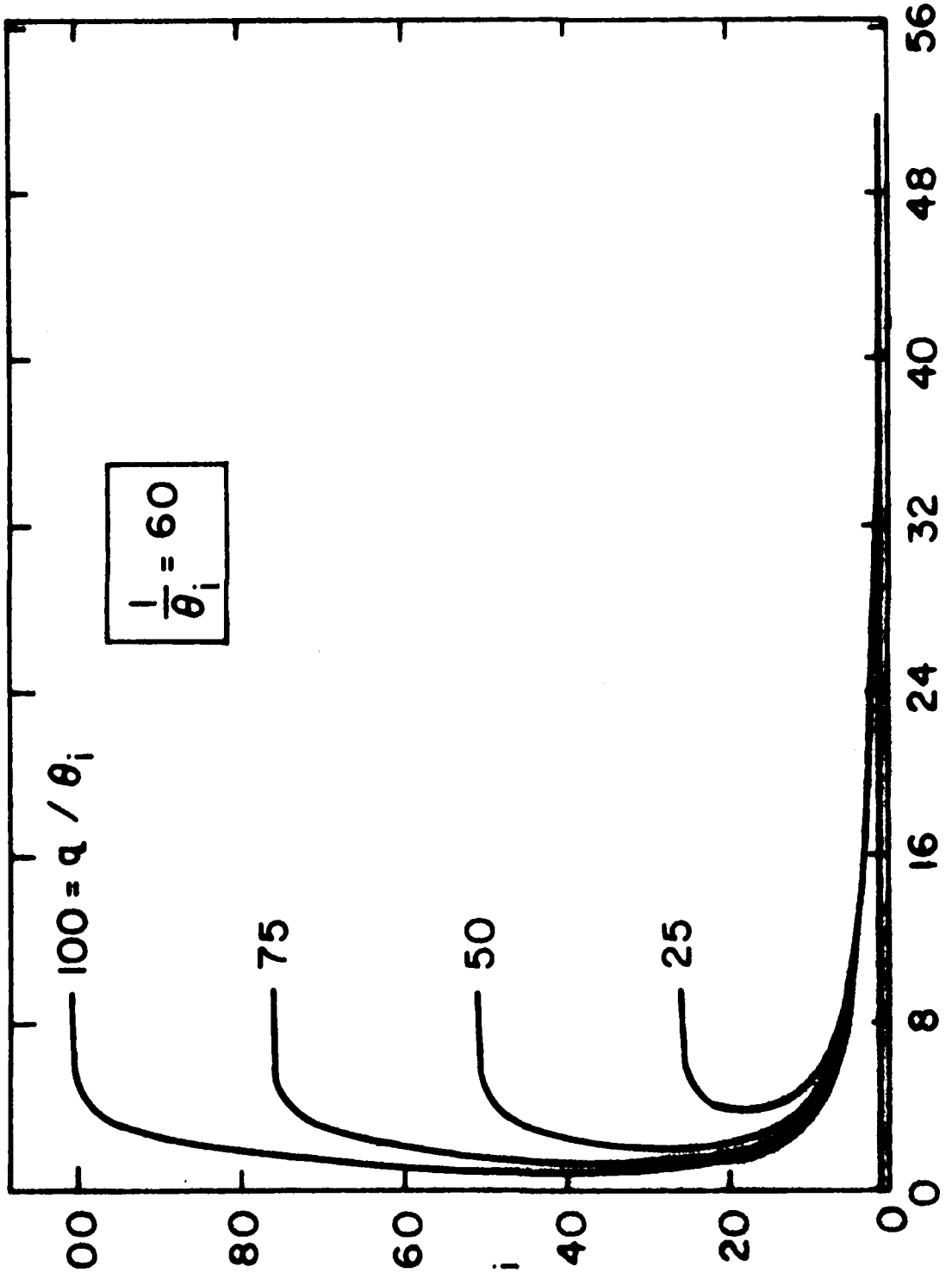

Figure 8. Reaction Temperature Dependence on Damkohler Number When Activation Energy is High.

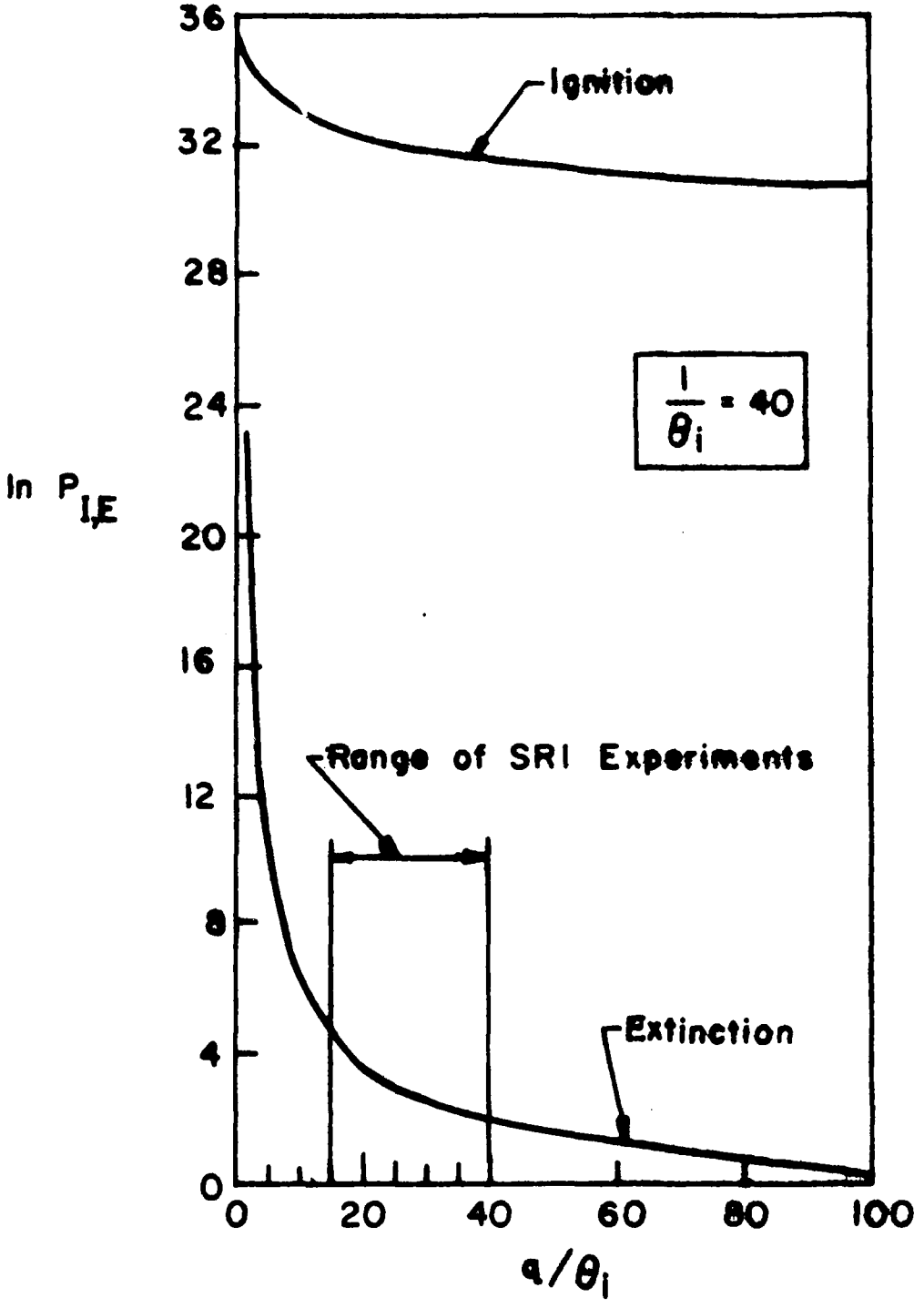

Figure 9. Map of Limiting Damkohler Number for Ignition and Extinction conditions: Inverse of Blast Strength, $P_{I,E}$ versus Fire Strength, q.

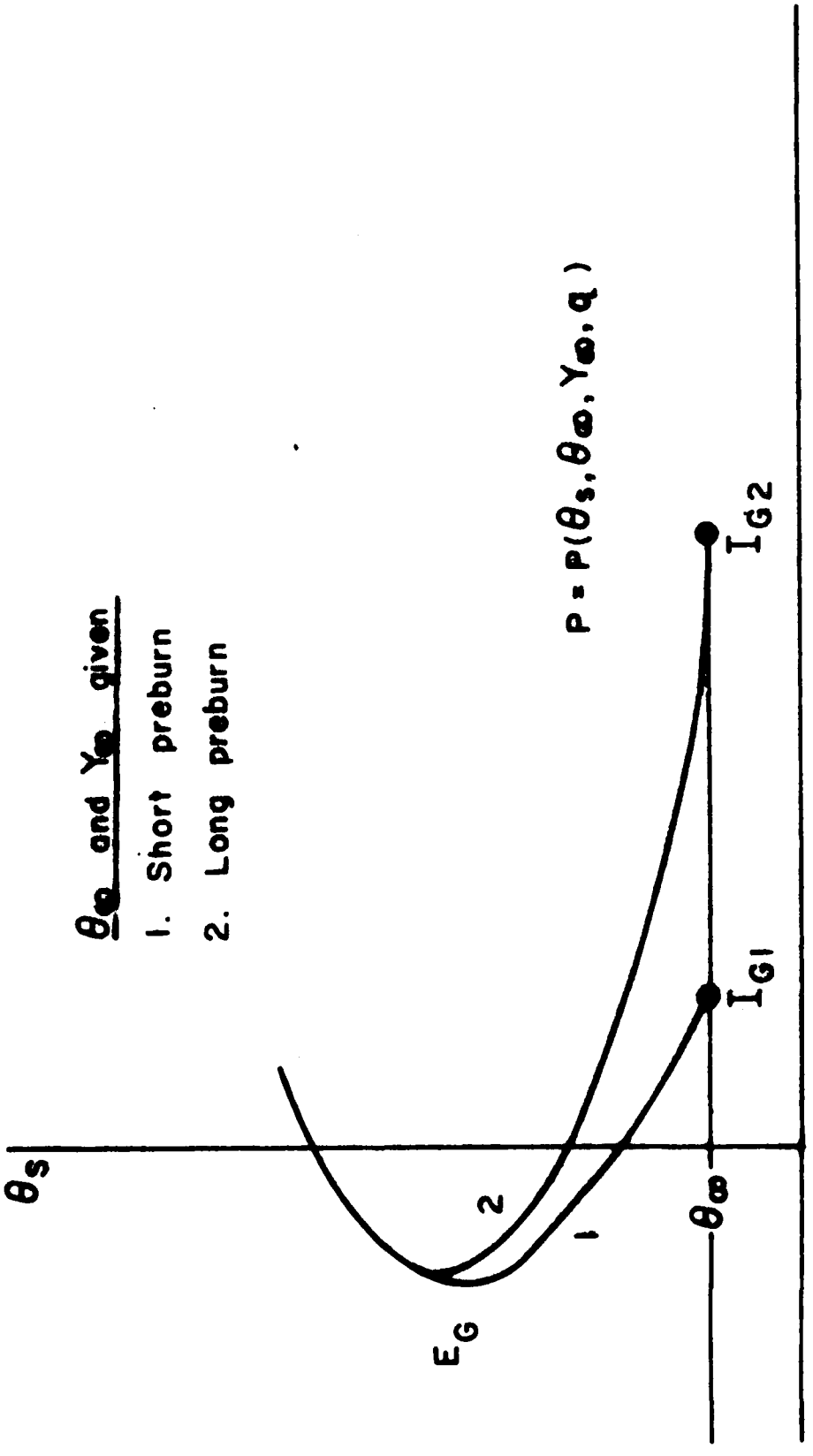

Figure 10. Effect of Preburn Time on the Wood Char Quality.

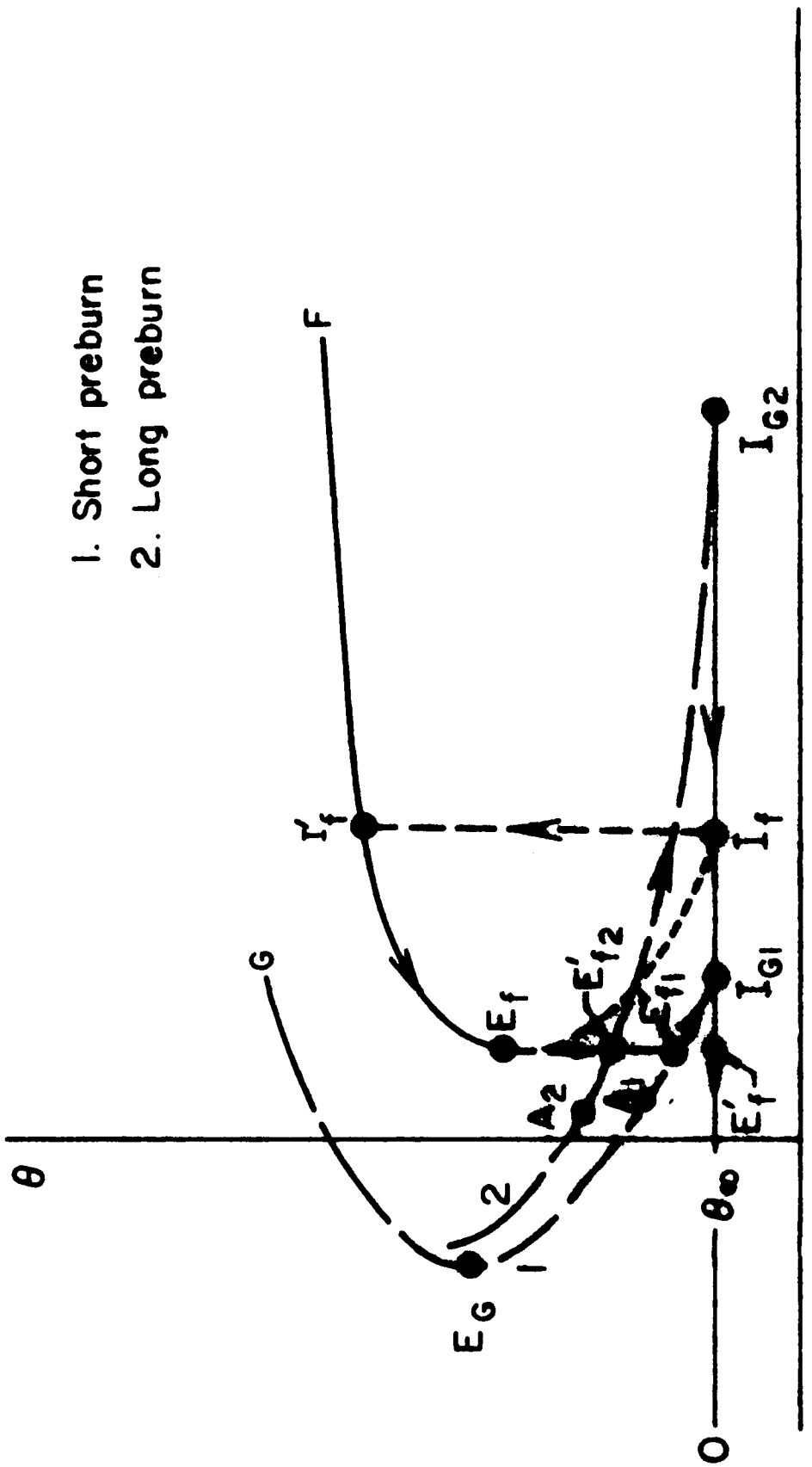

Figure 11. Mechanism of Extinction and Reignition of Flames on Charring Solids.

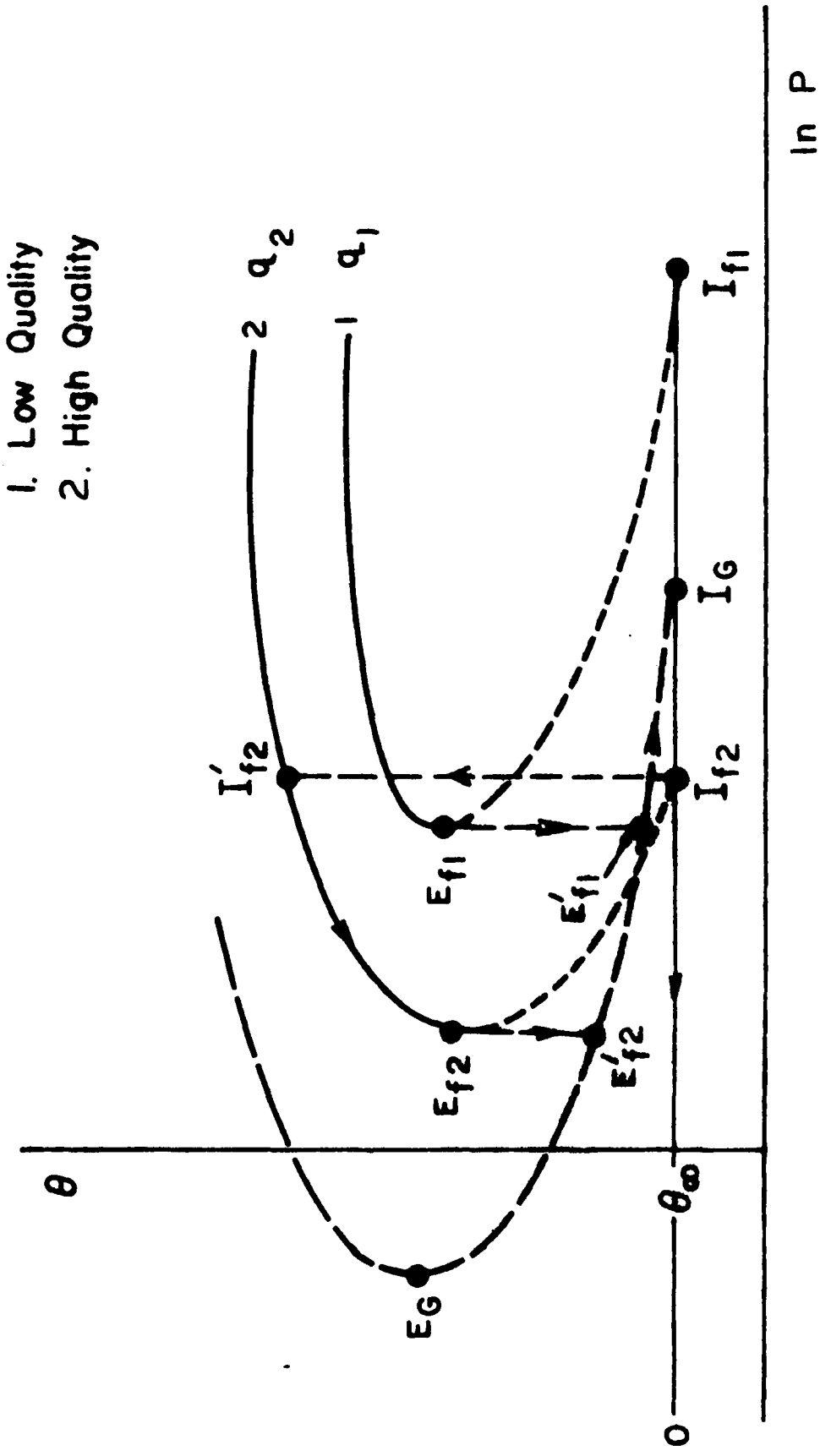

Figure 12. Effect of the Pyrolyzate Quality Upon Extinction and Reignition of Flames on Charring Solids.

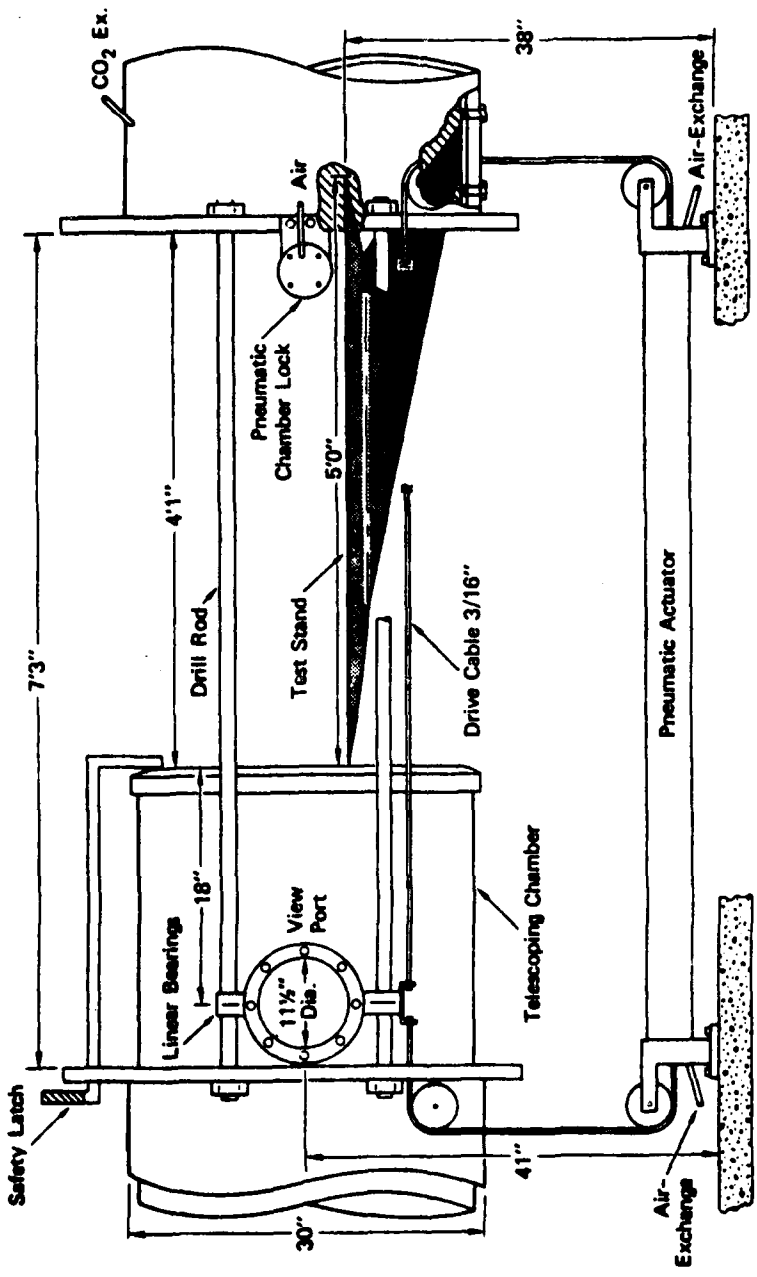

Figure 13: The SRI Shocktube Test Section Detail

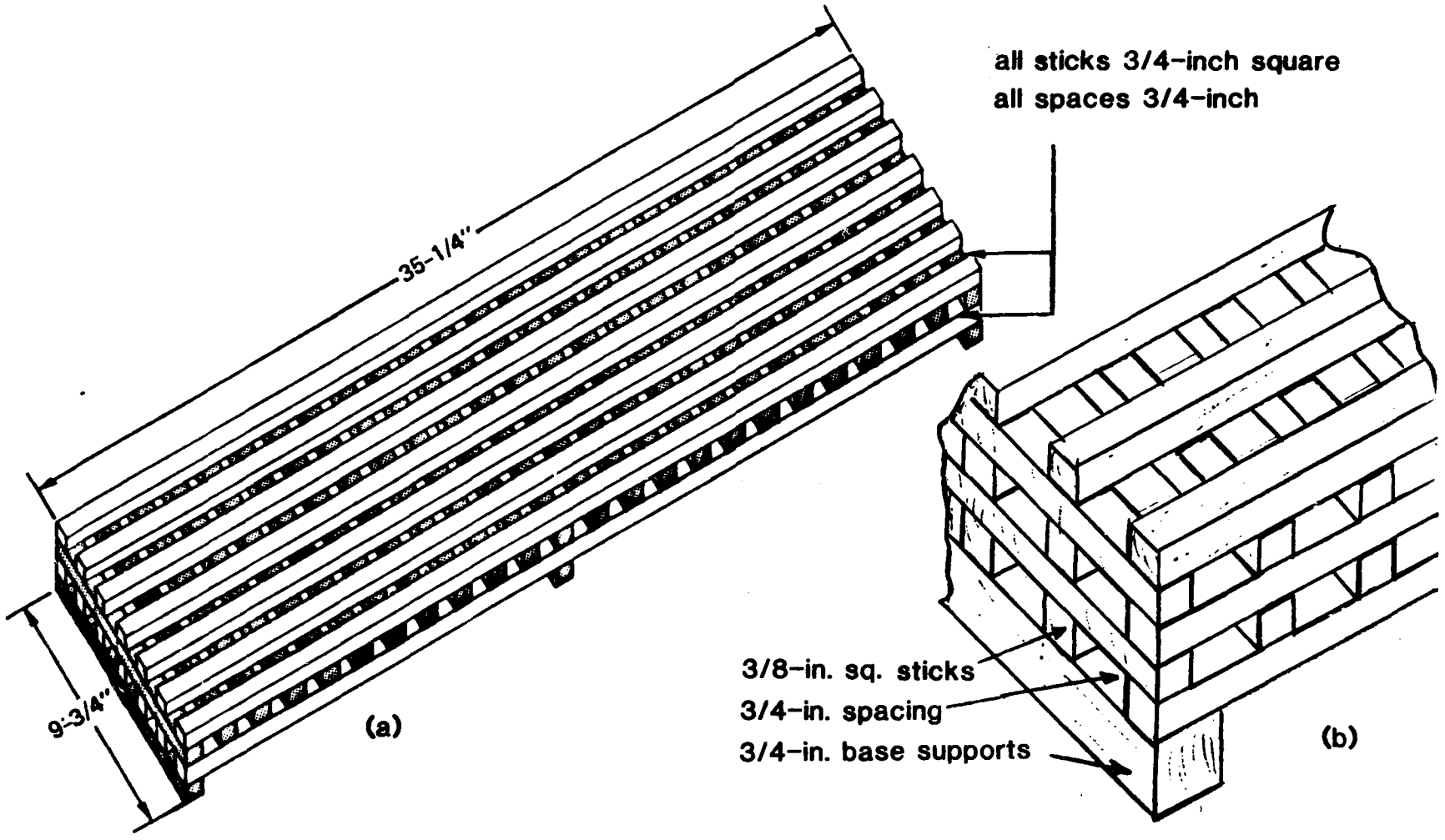

Figure 14: SRI Wood Crib Designs: (a) 3/4-inch Stick Crib, and (b) Detail of 3/8-inch Stick Crib.

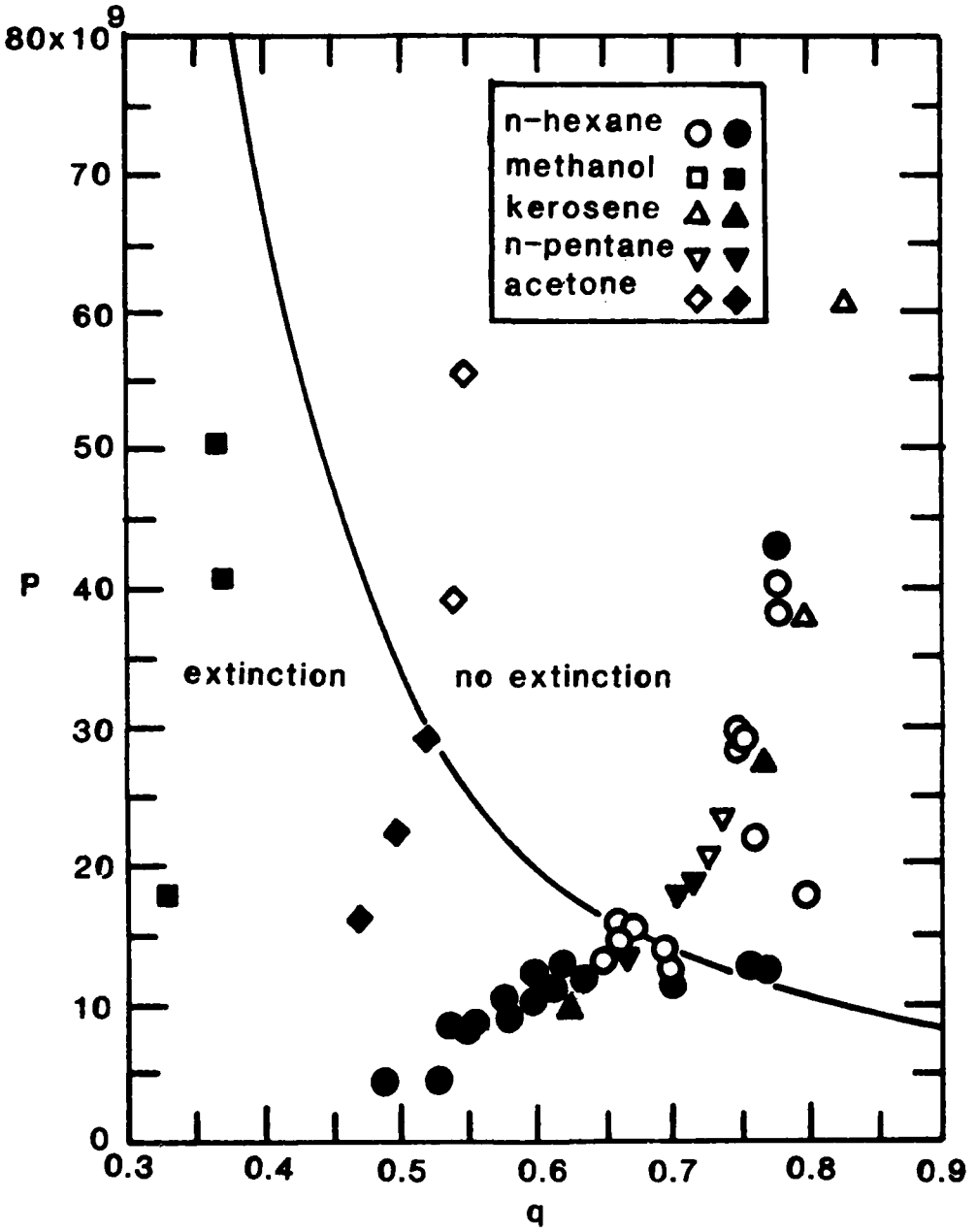

Figure 15: Extinction (filled symbols) – No Extinction (open symbols) Coorrelation for Class B Fires with No Barriers.

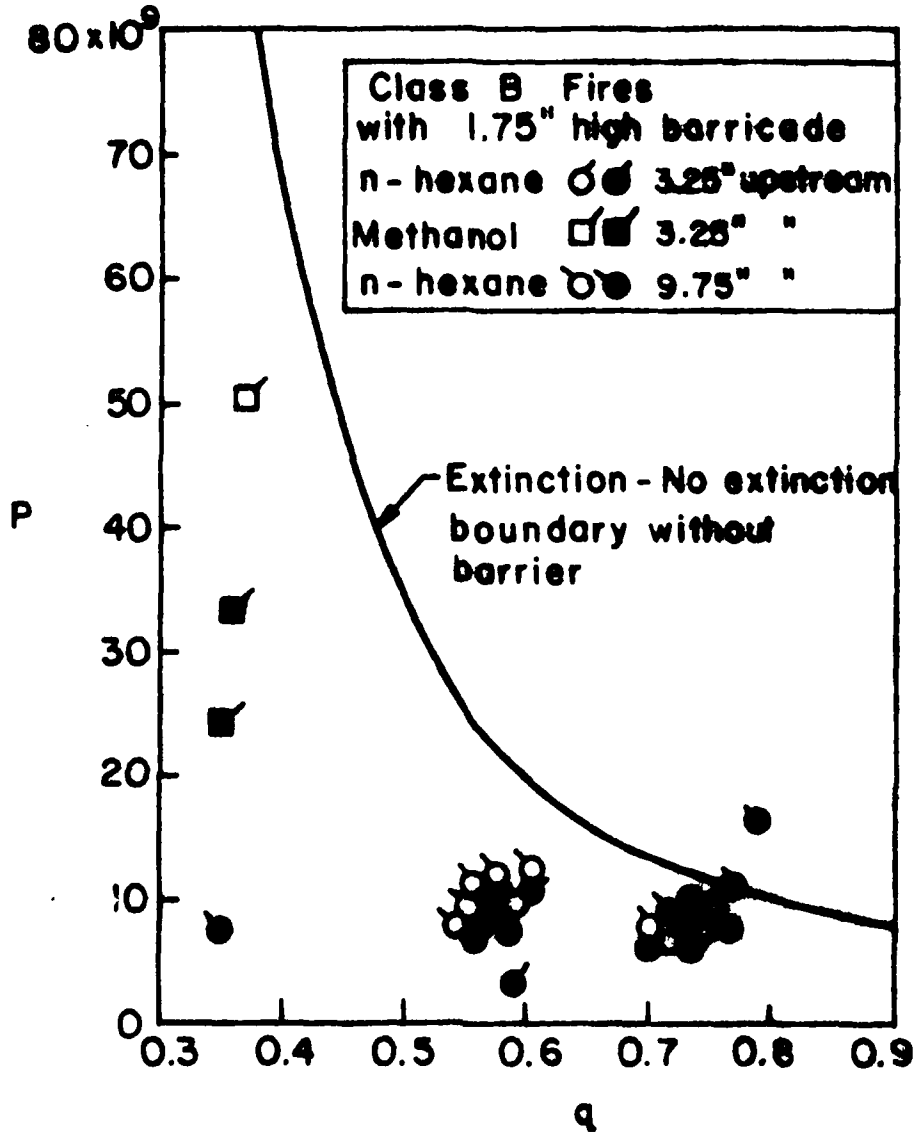

Figure 16. Test of the Hypothesis for the Effect of Barricade on Class B Fires.

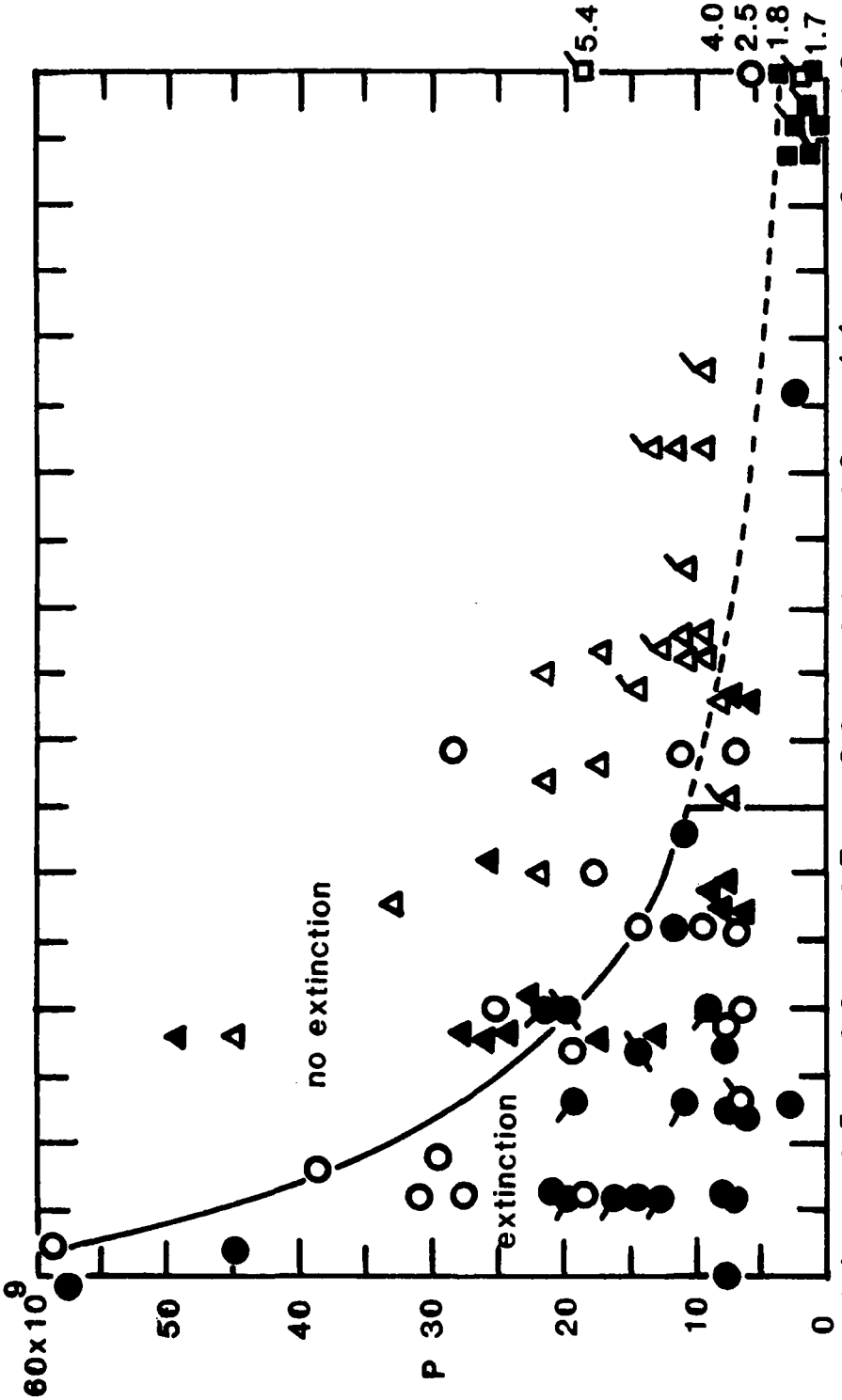

3/4" stick cribs: ● extinguished. ○ sustained. ◗ extinguished, glows, no reflash. ◪ extinguished, close to reflash. ◎ reflashed.

3/8" stick cribs: ▲ extinguished. △ sustained. ◭ reflashed.

shredded paper trays: ■ extinguished. □ sustained. ◫ rekindled. ◪ rekindled upon blowing air.

Figure 17: Extinction– No Extinction Correlation of Class A Fires.

TABLE 1

(Table 1 of Ref. 1)

SUMMARY OF HEXANE TEST RESULTS

Test No.	Substrate	Fuel Bed Length (inches)	Est. Peak Over-Pressure (psi)	Positive Phase Duration (sec)	Computed* Air Displacement (ft)	Observation	h_c (MJ/kg)	q	P
3	rock	24	9	[illegible]		fire out	44.75	0.53	4.94×10^9
4	rock	36	8	3.0	440.0	fire out	"	0.55	8.17 "
5†	rock	36	8	3.8	520.0	fire out	"	0.55	8.17 "
6†	rock	24	∿ 11(nc)	3.8		fire out, but see text	"	0.49	4.19 "
7	rock	36	1.3	0.65	35.0	fire out	"	0.78	43.00 "
8	rock	36	∿ 2	0.35	8.2	fire sustained	"	0.75	28.50 "
10	firebrick	36	1.4	0.3		fire sustained	"	0.78	40.10 "
14	firebrick	36	∿ 8	0.2	33.0	fire out	"	0.55	8.17 "
15	firebrick	12	1.5	0.07	5.2	fire out	"	0.77	12.50 "
16	firebrick	24	1.7	0.15	8.0	fire sustained	"	0.76	22.20 "
17	firebrick	36	5.2	0.25	23.0	fire out	"	0.63	11.90 "
19**	kaowool M board	36	2.0	0.175		fire sustained			
20**	kaowool M board	36	4.3	0.28		fire sustained			
21**	kaowool M board	36	5.9	0.275		fire out			
22**	kaowool M board	36	5.2	0.31		fire out			
23**	kaowool M board	24	2.9	0.29		fire sustained			
24**	kaowool M board	24	3.6	0.135		fire out			
25**	kaowool M board	12	1.8	0.07		fire out			
26**	kaowool M board	12	1.2	0.07		fire sustained			
27	kaowool M board	12	NA	NA		fire sustained			
28	kaowool M board	12	NA	NA		fire sustained			

*Computed as $50 \cdot \int_0^{t_+} p(t)dt$; where p(t) is the pressure-time record at the test section (in psi) and t_+ is duration of the positive phase of that record.

†Test with barrier.

nc - Nonclassical waveform

NA - Test run with line charge only, no plenum pressure.

** These tests are rereported in Ref. 2. See Table 2.

TABLE 2

(Table B.1 of Ref. 2)

CLASS-B FUEL TESTS - NO BARRIER

Test No.	Fuel	Bed Length (inches)	Preburn Time (s)	Mean Over-pressure (psi)	Positive Phase Duration (ms)[a]	Observation	h_c (MJ/kg)	q	P*
21[b]	n-Hexane	36	30	6.77	172 (65)	Fire out	44.75	0.58	9.42×10^9
22[b]	n-Hexane	36	30	4.55	170 (60)	Fire sustained	"	0.65	13.30 "
20[b]	n-Hexane	36	30	4.23	170 (66)	Fire sustained	"	0.66	14.20 "
19[b]	n-Hexane	36	30	1.99	170 (60)	Fire sustained	"	0.75	28.60 "
33	n-Hexane	36	15	5.79	115 (58)	Fire out	"	0.61	10.80 "
34	n-Hexane	36	15	3.97	115 (63)	Fire sustained	"	0.67	15.10 "
35	n-Hexane	36	15	1.94	100 (60)	Fire sustained	"	0.75	29.40 "
36	n-Hexane	36	15	1.46	90 (60)	Fire sustained	"	0.78	38.50 "
23[b]	n-Hexane	24	30	3.11	150 (65)	Fire sustained	"	0.70	12.60 "
24[b]	n-Hexane	24	20	3.32	145 (59)	Fire out	"	0.70	11.80 "
25[b]	n-Hexane	12	20	1.57	110 (62)	Fire out	"	0.77	12.00 "
26[b]	n-Hexane	12	20	1.04	70 (68)	Fire sustained	"	0.80	17.80 "
37	Methanol	36	15	3.3	77 (55)	Fire out	21.16	0.33	17.90 "
38	Methanol	36	30	1.4	68 (62)	Fire out	"	0.37	40.10 "
40	Methanol	36	30	1.1	68 (61)	Fire out	"	0.37	50.60 "

[a] Numbers in parentheses represent the time over which pressure was averaged.

[b] Tests completed in 1979 and reported in Reference 1. See note in Table 1.

TABLE 3

(Table B-1 of Ref. 3)

CLASS B FUEL TESTS

Bed Length = 36 in.

Test No.	Fuel	Preburn Time	Mean Overpressure (psi)	Positive Phase Duration (ms)[a]	First Flashback (ms)[b]	Observation	h_c (MJ/kg)	q	P
1	Kerosene	15	5.59	135(57)	-	Fire out	46.00	0.63	11.1×10^9
2	Kerosene	15	2.06	108(61)	-	Fire out	"	0.77	27.7 "
3	Kerosene	15	0.91	107(61)	?	Fire sustained	"	0.83	60.9 "
4	Kerosene	15	1.49	109(61)	137	Fire sustained	"	0.80	37.8 "
5	n-Pentane	10	4.36	174(58)	-	Fire out	45.47	0.67	13.9 "
6	n-Pentane	5	2.42	175(60)	?	Fire sustained	"	0.74	23.8 "
8	n-Pentane	5	3.16	150(59)	-	Fire out	"	0.71	18.6 "
9	n-Pentane	5	2.80	159(57)	133	Fire sustained	"	0.73	20.8 "
10	n-Pentane	5	3.04	129(56)	-	Fire out	"	0.72	19.3 "
11	Acetone	15	3.60	74(59)	-	Fire out	30.87	0.47	16.5 "
12	Acetone	15	2.53	71(55)	-	Fire out	"	0.50	22.9 "
13	Acetone	15	1.94	70(62)	-	Fire out	"	0.52	29.4 "
14	Acetone	15	~1.0	71(60)	?	Fire sustained	"	0.55	55.5 "
15	Acetone	15	1.43	70(61)	~130	Fire sustained	"	0.54	39.3 "
32	n-Hexane	15	~6.2	>150	-	Fire out	44.57	0.60	10.2 "
33	n-Hexane	15	~4.0	>150	?	Fire sustained	"	0.67	15.0 "

[a] The increases in positive phase durations for kerosene, pentane, and hexane tests are caused by pressure increases due to fuel combustion during test. Numbers in parentheses represent the time over which pressure was averaged.

[b] Time measured from shock arrival at test section.

TABLE 4

(Table B.5 of Ref. 2)

NONSTANDARD TESTS

Test No.	Fuel	Bed Length (in)	Barr. Dist. (in)	Barr. Ht. (in)	Preburn Time (s)	Mean o.p. (psi)	Fire	Comments	h_c (MJ/kg)	q	P
65	n-Hexane	36	3.25	0.6	15	5.31	Out	Decreased barrier height	44.57	0.63	11.6×10^9
81	n-Hexane	36	4.625	0.875	15	7	Out	Same barricade height:distance	"	0.58	9.15 "
82	n-Hexane	36	4.625	0.875	15	6.25	Out	ratio as 1.75:9.25 inches.	"	0.60	10.10 "
83	None	24	—	—	—	∿ 3.25	Not lit	Hycam film coverage			
84	None	24	0	1.75	—	∿ 3.25	Not lit	Hycam film coverage			
85	None	24	3.25	1.75	—	∿ 3.25	Not lit	Hycam film coverage			
86	n-Hexane	24	3.25	1.75	15	∿ 3.25	Sustained	Hycam film coverage	"	0.70	12.10 "
87	None	—	(a)	1.75	—	∿ 3.6	—	Shadowgraph visualization of shock/ barrier interaction			
88	None	—	(a)	1.75	—	∿ 3.5	—	Particle flow visualization			
39	Methanol	36	—	—	30	—	Sustained	No tank pressure (detonation only); flame disturbed but not blown off			
67	Redwood crib	12	—	—	120	7.34	Out	Crib burned poorly		τ=0.53	2.93 "
68	Redwood crib	12	—	—	240	7.80	Out	Crib burned poorly		1.06	2.78 "
69	Redwood crib	24	—	—	900	8.14	Sustained	Full crib involvement; some loss of crib integrity		3.97	5.37 "

[a]Barrier was positioned 1.25-in. upstream from center of window.

Tests No. 31, 32, 51, 53, 66, 72, 73, 74, 75, 99: had no or improper diaphram rupture.
Tests No. 30, 48, 71, 78: had improper recorder function.
Test No. 70: Test stand and (Douglas fir, 34½-in. long) crib displacement due to high overpressure (11.6 psi).

TABLE 5

(Table B.2 of Ref. 2)

CLASS-B FUEL TESTS - Barrier Distance = 3.25 inches
- Barrier Height = 1.75 inches

Test No.	Fuel	Bed Length (inches)	Preburn Time (s)	Mean Over-Pressure (psi)	Positive Phase Duration (ms)[a]	Observation	h_c (MJ/kg)	q	P
44	n-Hexane	36	15	7.44	120 (61)	Fire out	44.75	0.57	8.69×10^9
45	n-Hexane	36	15	6.4	120 (60)	Fire sustained	"	0.59	9.89 "
46	n-Hexane	36	15	6.84	122 (60)	Fire out	"	0.58	9.34 "
55	n-Hexane	36	15	6.16	119 (58)	Fire out	"	0.60	10.20 "
54	n-Hexane	12	15	6.39	95 (57)	Fire out	"	0.59	3.30 "
58	n-Hexane	12	15	2.37	78 (58)	Fire out	"	0.73	8.10 "
59	n-Hexane	12	15	1.98	94 (58)	Fire sustained	"	0.75	9.60 "
60	n-Hexane	12	15	2.27	98 (61)	Fire sustained	"	0.74	8.44 "
41	Methanol	36	30	1.1	68 (61)	Fire sustained	21.16	0.37	50.60 "
42	Methanol	36	30	2.4	68 (57)	Fire out	"	0.35	24.00 "
43	Methanol	36	30	1.7	68 (58)	Fire out	"	0.36	33.30 "

[a]Numbers in parentheses represent the time over which pressure was averaged.

TABLE 6

(Table B.3 of Ref. 2)

CLASS B FUEL TESTS - Barrier Distance = 9.25 inches
- Barrier Height = 1.75 inches

Test No.	Fuel	Bed Length (inches)	Preburn Time (s)	Mean Over-Pressure (psi)	Positive Phase Duration (ms)[a]	Observation	h_c (MJ/kg)	q	p
47	n-Hexane	36	15	5.96	100 (60)	Fire sustained	44.75	0.61	10.5×10^9
49	n-Hexane	36	15	7.26	110 (60)	Fire sustained	"	0.57	8.87 "
50	n-Hexane	36	15	7.3	120 (62)	Fire out	"	0.57	8.83 "
52	n-Hexane	36	15	7.5	100 (60)	Fire sustained	"	0.56	8.63 "
56	n-Hexane	36	15	6.76	100 (60)	Fire sustained	"	0.58	9.43 "
57	n-Hexane	36	15	6.93	118 (60)	Fire out	"	0.58	9.23 "
76	n-Hexane	36	15	7.22	100 (58)	Fire sustained	"	0.57	8.92 "
61	n-Hexane	12(M)[b]	15	2.45	80 (57)	Fire out	"	0.35	7.85 "
62	n-Hexane	12(M)	15	1.94	72 (56)	Fire out	"	0.75	9.79 "
63	n-Hexane	12(M)	15	1.60	73 (56)	Fire out	"	0.77	11.80 "
64	n-Hexane	12(M)	15	1.12	71 (58)	Fire out	"	0.79	16.60 "
108	n-Hexane	12(M)	15	2.17	93 (58)	Fire out	"	0.74	8.80 "
77	n-Hexane	12(F)[c]	15	2.68	78 (57)	Fire sustained	"	0.72	7.22 "
79	n-Hexane	12(F)	15	2.61	82 (57)	Fire sustained	"	0.72	7.40 "
80	n-Hexane	12(F)	15	2.85	74 (56)	Fire out	"	0.71	6.82 "
109	n-Hexane	12(F)	15	2.51	93 (57)	Fire out	"	0.73	7.68 "
110	n-Hexane	12(F)	15	2.15	93 (58)	Fire out	"	0.74	8.88 "

[a] Numbers in parentheses represent the time over which the pressure was averaged.

[b] (M) means the middle position; i.e., the middle 1-foot section of the basic 3-foot bed was used as the fuel bed.

[c] (F) means the front position; i.e., the front (upstream) 1-foot section was used as the fuel bed.

TABLE 7

(Table B.4 of Ref. 2)

WOOD CRIB TESTS

(3/4 inch sticks)

Test No.	Preburn Time (s)	Estimated wt. loss (%)	Mean Over-pressure (psi)	Positive Phase Duration (ms)[a]	Observation	τ[d]	P'
89	90	9.5	8.56	93 (64)	Fire out	0.40	7.56×10^9
90	120	16.1	9.02	93 (58)	Fire out	0.53	7.24 "
91	180	–	9.14	95 (58)	Fire sustained	0.79	7.16 "
92	150	(35.0)	9.08	103 (56)	Fire sustained	0.66	7.20 "
93	120	(16.9)	9.39	103 (56)	Fire sustained (flame flashback)	0.53	7.00 "
94	105	9.3	8.24	95 (56)	Fire out (crib burned poorly)	0.46	7.81 "
95	105	10.8	8.88	95 (56)	Fire out	0.46	7.34 "
96	120	15.2	8.79	95 (58)	Fire out	0.53	7.40 "
97	105	9.4	4.05	85 (57)	Fire out (crib burned poorly) (bad diaphram rupture)	0.46	14.50 "
98	105	(14.0)	3.06	117 (57)	Fire sustained	0.46	18.80 "
100	105	10.8	3.7	81 (57)	Fire out (crib glows after test)	0.46	15.80 "
101	105	10.2	4.35	83 (56)	Fire out (crib glows brightly)	0.46	13.60 "
102	105	12.6	2.84	80 (56)	Fire out (no glow *visible*)	0.46	20.10 "
103	105	(14.4)	1.80	73 (56)	Fire sustained	0.46	30.90 "
104	105	(13.1)	2.0	72 (57)	Fire sustained	0.46	27.90 "
105	105	13.2	2.97	78 (57)	Fire out (crib glows brightly)	0.46	19.30 "
106	120	17.8	2.93	103 (57)	Fire out (crib glows after test)	0.53	19.50 "
107	135	22.8	2.9	103 (56)	Fire out (crib close to relighting)	0.60	19.70 "
111	120	18.4	5.58	85 (53)	Fire out (crib glows after test)	0.53	10.90 "
112	150	24.4	5.3	83 (56)	Fire out/but relighted after door opened ~ 15 sec	0.66	11.40 "
113	180	(35.7)	5.36	81 (56)	Fire sustained	0.79	11.30 "
114	150	(27.7)	6.93	90 (56)	Fire sustained	0.66	9.04 "
115	165	23.6	5.45	95 (57)	Fire out/but relighted after removal	0.73	11.10 "
116	135	21.9	6.73	82 (57)	Fire out (crib glows after test)	0.60	9.27 "
117	150	(29.3)	4.18	83 (57)	Fire sustained	0.66	14.10 "
118	130	20.3	4.11	83 (60)	Fire out/but close to relighting	0.57	14.30 "
119	130	(23.3)	3.0	82 (58)	Fire sustained	0.57	19.10 "
120	135	22.5	2.82	81 (56)	Fire out (crib glows after test)	0.60	20.20 "
121	135	(24.4)	2.23	80 (58)	Fire sustained	0.60	25.20 "
122	180	(33.2)	1.95[c]	1400	Fire sustained	0.79	28.60 "
123	110	(14.3)	1.9[c]	3200	Fire sustained	0.49	29.30 "
124	160	(28.1)	3.25[c]	4000	Fire sustained	0.70	17.70 "

[a] Numbers in parentheses represent the time over which pressure was averaged.

[b] Numbers in parentheses represent weight loss after extinction with CO_2.

[c] Pressure history for the long-duration pressure pulses is shown in Figure 5.

[d] $\tau \equiv 2.7\ t_{preburn}/t^*$; $t^* \equiv 612$ s.

TABLE 8

(Table B-3 of Ref. 3)

WOOD CRIB TESTS

(3/4 in. Stick Cribs)

Test No.	Crib Weight (g)	Preburn Time (s)	Measured Wt. Loss (%)	Mean Blast Over Pressure (psi)	Observation	τ^d	P
76	3864	135	23.3	9.55	Fire sustained	0.60	6.91×10^9
77	3608	128.4	14.2	9.04	Fire out	0.57	7.23 "
78	3428	134	16.9	8.7	Fire sustained	0.59	7.46 "
82	3670	96	6.8	0.91	Fire sustained	0.42	59.60 "
83	3658	95.6	5.9	1.24	Fire out	0.42	44.10 "
84	3391	89.5	5.9	0.95	Fire out	0.39	57.20 "
85	3432	108	9.3	1.43	Fire sustained	0.48	38.50 "

[b] $\tau \equiv 2.7\ t_{preburn}/t^\circ$; $t^\circ = 612$ s.

TABLE 9

(Table B-2 of Ref. 3)

WOOD CRIB TESTS

(3/8-in. Stick Cribs)

Test No.	Crib Initial Weight (g)	Preburn Time (s)	Approx. Measured Wt. Loss (%)	Mean Overpressure (psi)	Observation	τ[b]	P
50	1788	111	(42.9)	6.92	Fire sustained (reignition)	1.08	9.05×10^9
51	1569	107	(61.4)	5.91	Fire sustained (reignition)	0.93	10.30 "
52	1559	88	(44.3)	6.88	Fire sustained	0.86	9.10 "
53	1683	88	(28.8)	5.88	Fire sustained	0.86	10.40 "
57	1698	60	15.3	4.57	Fire out	0.58	13.00 "
58	1731	60	15.1	3.05	Fire out	0.58	18.80 "
59	1755	60	12.8	2.02	Fire out	0.58	27.60 "
60	1783	60	15.7	1.24	Fire sustained	0.58	44.10 "
61	1740	73	19.3	2.21	Fire out	0.71	25.40 "
62	1878	72	17.3	1.69	Fire sustained	0.68	32.60 "
63*	1670	71	12.8	7.17	Fire out	0.69	8.78 "
64*	1669	91	(60.9)	6.75	Fire sustained	0.88	9.25 "
65*	1704	85	31.0	7.90	Fire sustained	0.83	8.09 "
66*	1708	70	14.1	7.92	Fire out	0.68	8.07 "
67*	1673	85	23.9	7.98	Fire out	0.83	8.02 "
68*	1693	85	25.1	9.88	Fire out	0.83	6.72 "
70*	1768	87	31.6	2.64	Fire sustained	0.85	21.50 "
71*	1780	62.5	13.1	2.56	Fire out	0.61	22.10 "
72*	1624	79	34.3	2.66	Fire sustained	0.77	21.40 "
73*	1706	72	21.1	2.60	Fire sustained	0.70	21.80 "
74*	1752	80	25.5	3.31	Fire sustained	0.78	17.40 "
75*	1750	86.5	33.0	4.10	Fire sustained (reignition)	0.84	14.40 "
79*	1742	69	18.2	9.05	Fire out	0.67	7.22 "
80*	1769	71	17.2	8.88	Fire out	0.69	7.34 "
81*	1781	78	25.0	8.77	Fire sustained (reignition)	0.76	7.41 "
39	1820	60†	7.7	2.16	Fire out	0.58	26.0×10^9
40	1741	60†	9.8	2.27	Fire out	0.58	24.8 "
41	1891	60†	9.0	1.11	Fire out	0.58	49.1 "
42	1900	90†	(46.6)	3.40	Fire sustained	0.87	17.0 "
43	1822	90†	27.0	5.77	Fire out	0.87	10.6 "
45	1842	90†	(32.1)	4.82	Fire sustained (reignition)	0.87	12.4 "
46	1843	105†	21.1	4.47	Fire sustained (reignition)	1.02	13.3 "
47	1710	105†	35.7	4.89	Fire sustained	1.02	12.3 "
49	1745	105†	(60.0)	6.89	Fire sustained	1.02	9.08 "

*Crib center support stick was removed.

†Slower burning cribs--unframed wick slowed down ignition

[b] $\tau = 2.7\ t_{preburn}/t^*$; $t^* = 278$ s.

TABLE 10

(Table B-4 of Ref. 3)

DEBRIS FIRE TESTS

(0.022-inch thick shreds)

Test No.	Fuel/ Fuel Arrangement Type[a]	Burner-on Period (s)	Total Preburn Time (s)	Mean Over-Pressure (psi)	Observations			τ[b]	F
					Fire Out?	Residual Smolder Present?	Did Fire Rekindle?		
1A	Blotter paper/A	?	?	10.	Yes	Yes	No	?	4.52×10^9
2A	Blotter paper/A	14	14	10.	Yes	Yes	No	2.52	4.52 "
4A	Blotter paper/A	9.8	9.8	3.5	Yes	?	Yes, after 15 sec	1.76	1.12 "
5A	Blotter paper/A	9.5	9.5	3.5	Yes	-	No	1.71	1.12 "
6A	Blotter paper/A	30	30	2.	Yes	?	Yes, after 10 sec	5.40	19.00 "
7A	Blotter paper/B	7	9	7.	Yes	Minor	No	1.26	1.53 "
8A	Blotter paper/B	7	14.5	3.5	Yes	Yes	Yes, with blowing	1.26	2.80 "
9A	Blotter paper/B	7	15.7	7.	Yes	Localized	Yes, with blowing	1.26	1.53 "
10A	Filter paper/B	7	14.5	7.	Yes	Little	No	1.26	1.53 "
11A	Filter paper/B	7	14.5	3.5	Yes	Some	No	1.26	2.80 "
12A	Filter paper/B	7	14.4	1.75	No	Yes	Probably	1.26	5.40 "

[a] Fuel Arrangement Type A: 2 ft. by 9 3/4 in. pan (2 1/2 in. deep)
Fuel Arrangement Type B: 6 in. by 10 in. tray (1 in. deep)

[b] $\tau \equiv 2.7\ t_{preburn}/t^*$, $t^* = 15$ sec.

UNIVERSITY OF NOTRE DAME, NOTRE DAME, IN 46556

RESPONSE MECHANISMS, BLAST/FIRE INTERACTION by A. Murty Kanury, 70 pages, FEMA contract No. EMW-C-0366, FEMA WORK UNIT 2564H, Unclassified. (November 1983).

Hypotheses are formulated of the process of interaction between an airblast and fires supported by liquid fuels and wood cribs. A map of blast weakness versus fire strength is conceived on which the regime of fire extinction can be delineated from the regime where the fire sustains the blast. The fire strength is described for liquid fuels primarily by the heat of combustion; and for wood, it is mainly described by the preburn time. The concept is substantiated by the SRI shock tube data.

UNIVERSITY OF NOTRE DAME, NOTRE DAME, IN 46556

RESPONSE MECHANISM: BLAST/FIRE INTERACTION by A. Murty Kanury, 70 pages, FEMA contract No. EMW-C-0366, FEMA WORK UNIT 2564H, Unclassified. (November 1983)

Hypotheses are formulated of the process of interaction between an airblast and fires supported by liquid fuels and wood cribs. A map of blast weakness versus fire strength is conceived on which the regime of fire extinction can be delineated from the regime where the fire sustains the blast. The fire strength is described for liquid fuels primarily by the heat of combustion; and for wood, it is mainly described by the preburn time. The concept is substantiated by the SRI shock tube data.

UNIVERSITY OF NOTRE DAME, NOTRE DAME, IN 46556

RESPONSE MECHANISMS, BLAST/FIRE INTERACTION by A. Murty Kanury, 70 pages, FEMA contract No. EMW-C-0366, FEMA WORK UNIT 2564H, unclassified. (November 1983).

Hypotheses are formulated of the process of interaction between an airblast and fires supported by liquid fuels and wood cribs. A map of blast weakness versus fire strength is conceived on which the regime of fire extinction can be delineated from the regime where the fire sustains the blast. The fire strength is described for liquid fuels primarily by the heat of combustion; and for wood, it is mainly described by the preburn time. The concept is substantiated by the SRI shock tube data

UNIVERSITY OF NOTRE DAME, NOTRE DAME, IN 46556

RESPONSE MECHANISM: BLAST/FIRE INTERACTION by A. Murty Kanury, 70 pages, FEMA contract No. EMW-C-0366, FEMA WORK UNIT 2564H, unclassified. (November 1983)

Hypotheses are formulated of the process of interaction between an airblast and fires supported by liquid fuels and wood cribs. A map of blast weakness versus fire strength is conceived on which the regime of fire extinction can be delineated from the regime where the fire sustains the blast. The fire strength is described for liquid fuels primarily by the heat of combustion; and for wood, it is mainly described by the preburn time. The concept is substantiated by the SRI shock tube data.

DISTRIBUTION LIST

Federal Emergency Management Agency
Attn: Jim Kerr, Director for Research
National Preparedness Programs
Directorate
Washington, DC 20472 (3 copies)

Federal Emergency Management Agency
Attn: Henry Tovey
Office of Research
National Preparedness Programs
Directorate
Washington, DC 20472 (45 copies)

Defense Technical Information Center
(DTIC)
Cameron Station
Alexandria, VA 22314 (12 copies)

Oak Ridge National Laboratory
Attn: Librarian
Post Office Box X
Oak Ridge, TN 37830

Los Alamos Scientific Laboratory
Attn: Document Library
Los Alamos, NM 87544

The RAND Corporation
Attn: Document Library
1700 Main Street
Santa Monica, CA 90406

Director, U.S. Army Engineer Waterways
Experiment Station
Attn: Document Library
P.O. Box 631
Vicksburg, MS 39180

Director, Army Materials and Mechanics
Research Center
Attn: Technical Library
Watertown, MA 02172

Director, US Army Ballistic Research
Laboratory
Attn: Document Library
Aberdeen Proving Ground, MD 21006

Director, U.S. Army Ballstic Research
Laboratory
Attn: Mr. William Taylor
Aberdeen Proving Ground, MD 21006 (2 copies)

U.S. Army Training and Doctrine
Command
Fort Monroe
Hampton, VA 23651

U.S. Army Combined Arms Combat
Development Activity
Fort Leavensworth, KS 66027

Air Force Weapons Laboratory
Attn: SUL Technical Library
Kirtland Air Force Base
Albuquerque, NM 87117

Air Force Weapons Laboratory
Attn: Civil Engineering Division
Kirtland Air Force Base
Albuquerque, NM 87117

Civil Engineering Center/AF/PRECET
Wright Patterson
Air Force Base, OH 45433

Chief of Engineers
Department of the Army
Attn: DAEN-RDZ-A
Washington, DC 20310

Assistant Secretary of the Army
(RD&A)
Attn: Deputy ASA for (RD&S)
Washington, DC 20310

Commanding Officer
U.S. Naval C.E. Laboratory
Attn: Document Library
Port Hueneme, CA 93401

Chief of Naval Research
Washington, DC 20306

Command and Control Technical
Center
Department of Defense
The Pentagon
Washington, DC 20301

Assistant Director
Energy and Natural Resources
Office of Science and Technology
Policy
Executive Office Building
Washington, DC 20500

Director
Department of Military Application
Department of Energy
Washington, DC 20545

Director
Defense Nuclear Agency
Attn: Michael Frankel
Washington, DC 20305

Director, Defense Nuclear Agency
Attn: Tom Kennedy
Washington, DC 20305

Dr. E. Sevin
Defense Nuclear Agency
6901 Telegraph Road
Alexandria, VA 22310

Director, Defense Nuclear Agency
Attn: Technical Library
Washington, DC 20305

Oak Ridge National Laboratory
Attn: Emergency Technology
Division Librarian
P.O. Box X
Oak Ridge, TN 37380

Director
Forest Fire & Atmospheric Science
Research
U.S. Forest Service
Department of Agriculture
Washington, DC 20013

Mr. Raymond Alger
SRI International
333 Ravenswood Avenue
Menlo Park, CA 94025

Mr. Normal J. Alvares
Lawrence Livermore National
Laboratory
University of California
P.O. Box 808, L-442
Livermore, CA 94550

Hal E. Anderson
USDA Forest Service
Intermountain Forest and Range
Experiment Station
Northern Forest Fire Laboratory,
Drawer G
Missoula, MT 59806

Gunnar Arbman
Swedish National Defense Research
Institute
Box 27322
S-10254 Stockholm, SWEDEN 631500

Donald Bettge
Federal Emergency Management
Agency
National Preparedness Programs
Directorate
Washington, DC 20472

Art Broyles
Lawrence Livermore National
Laboratory
University of California
P.O. Box 808, L-10
Livermore, CA 94550

Dr. Jana Backovsky
SRI International
333 Ravenswood Avenue
Menlo Park, CA 94025

Mr. Clay P. Butler
SRI International
333 Ravenswood Avenue
Menlo Park, CA 94025

Dr. Barry Bowman
Lawrence Livermore National
Laboratory
University of California
P.O. Box 808
Livermore, CA 94550

Bell Telephone Laboratories
Attn: Mr. E. Witt
Mr. R. May
Mr. J. Foss
Whippany Road
Whippany, NJ 07981 (3 copies)

H.L. Brode
Pacific-Sierra Research Corp.
12340 Santa Monica Boulevard
Los Angeles, CA 90025

W. Baker
Southwest Research Institute
P.O. Drawer 2851D
San Antonio, TX 78284

Mr. A.P. Brackebush
Forest Fire Research
Northern Forest Fire Laboratory
Missoula, MT 59801

U.S. Forest Service
Attn: Dr. A. Broido
P.O. Box 245
Berkeley, CA 94710

Dr. Cagliostro
MS-K555, P.O. Box 1663
Los Alamos Scientific Laboratory
Los Alamos, NM 87544

George Carr-Hill
Home Office
Scientific Advisory Branch
Horseferry House
Dean Ryle Street
London SWIP 2AW, ENGLAND

Edward J. Chapyak
Energy Division
Los Angeles National Laboratory, MS K559
P.O. Box 1663
Los Alamos, NM 87545

Dr. Conrad Chester
Oak Ridge National Laboratory
P.O. Box X
Oak Ridge, TN 37380

George Coulter
U.S. Army Ballistic Research Laboratory
U.S. Army Armament Research and
Development Command
Aberdeen Proving Ground, MD 21005

Dr. John Cockayne
Senior Scientist
Science Applications, Inc.
1710 Goodrige Drive
P.O. Box 1303
McLean, VA 22101

Director, U.S. Army Engineering Waterways
Experiment Station
Attn: Mr. W.I. Huff
P.O. Box 631
Vicksburg, MI 39180

Dr. William F. Christian
Underwriters' Laboratories, Inc.
333 Pfingsten Road
Northbrook, IL 60062

L. Lynn Cleland
Lawrence Livermore National
Laboratory
University of California
P.O. Box 808, L-91
Livermore, CA 94550

Garth E. Cummings
Lawrence Livermore National
Laboratory
University of California
P.O. Box 808, L-91
Livermore, CA 94550

Dr. William Chenault
Human Sciences Research, Inc.
Westgate Industrial Park
7710 Old Springhouse Road
McLean, VA 22102

Dikewood Corporation
1613 University Boulevard, N.E.
Albuquerque, NM 87102

Terry R. Donich
Lawrence Livermore National
Laboratory
University of California
P.O. box 808, L-97
Livermore, CA 94550

Mr. Marvin Drake
Science Applications, Inc.
1200 Prospect Street
La Jolla, CA 92037

John de Ris
Factory Mutual Research Corp.
Norwood, MA 02062

Mr. Donald Drzewiecki
Calspan Corporation
P.O. Box 400
Buffalo, NY 14225

University of Florida
Civil Defense Technical Services Center
College of Engineering
Department of Engineering
Gainesville, FL 32601

Dr. Francis E. Fendell
R1/1038
TRW
One Space Park
Redondo Beach, CA 90278

Mr. Dick Foster
SRI International
1611 Kent Street
Arlington, VA 22209

Mr. Robert Fristrom
John Hopkins Applied Physics
Laboratory
John Hopkins Road
Laurel, MD 20707

Factory Mutal Research Corporation
Attn: Dr. Ray Friedman
1151 Boston-Providence Turnpike
Norwood, MA 02062

Fire Research Library
National Bureau of Standards
Building 224 - Room A-246
Washington, DC 20234

B. Gabrielsen
Scientific Service, Inc.
517 East Bayshore Drive
Redwood City, CA 94060

Laurence L. George
Lawrence Livermore National Laboratory
University of California
P.O. Box 808, L-140
Livermore, CA 94550

Dr. Matthew G. Gibberts
5424 Lawton Avenue
Oakland, CA 94618

Paul J. Hassig
California Research & Technology,
Inc.
20943 Devonshire Street
Chatsworth, CA 91311

Robert G. Hickman
Lawrence Livermore National
Laboratory
University of California
P.O. Box 808, L-140
Livermore, CA 94550

Mr. Edward L. Hill
Research Triangle Institute
P.O. Box 12194
Research Triangle Park, NC 27709

Dr. Dennis HOlliday
R&D Associates
P.O. Box 9695
Marina Del Rey, CA 90291

Mr. W.L. Huff
USAE Waterways Experiment Station
Post Office Box 631
Vicksburg, MI 39180

Mr. Peter S. Hughes
Los Alamos Technical Associate,
Inc.
P.O. Box 410
Los Alamos, NM 87544 (2 copies)

Hudson Institute
Quaker Ridge Road
Croton-on-Hudson, NY 10520

Applied Research and Associates
Attn: Cornelius J. Higgins
2601 Wyoming Blvd., Suite H-1
Albuquerque, NM 87112

Mr. Kenneth Kaplan
#30 White Plains Court
San Mateo, CA 94402

Sang-Wook Kang
Lawrence Livermore National
Laboratory
University of California
P.O. Box 808, L-140
Livermore, CA 94550

Edward J. Kansa
Lawrence Livermore National
Laboratory
University of California
P.O. Box 808, L-451
Livermore, CA 94550

Sam A. Kiger
ISAE Waterways Experiment Station
Vicksburg, MS 39180

Chi-Yung King
Lawrence Livermore National Laboratory
University of California
P.O. Box 808, L-799
Livermore, CA 94550

Professor A. Murty Kanury
Department of Aerospace and Mechanical Engineering
University of Notre Dame
Notre Dame, IN 46556

Mr. Samuel Kramer
National Bureau of Standards
Building 225 - Room B-124
Washington, DC 20234

Mr. Richard Laurino
Center for Planning and Research
2483 East Bayshore, Suite 104
Palo Alto, CA 94303

Mr. Jud Leech
BDM Corporation
1801 Randolph Road, S.E.
Albuquerque, NM 87106

Dr. Anatole Longinow
IIT Research Institute
10 West 35th Street
Chicago, IL 60616

Director
Lovelace Foundation
5200 Gibson Boulevard, SE
Albuquerque, NM 87108

Harold J. Linnerud
Science and Engineering Associates Inc.
16 Westford Street
Chelmsford, MA 01824

R. Levine
National Bureau of Standards
B260 - 224
Washington, DC 20234

Mr. Stanley B. Martin
Stan Martin and Associates
869 Vista Drive
Redwood City, CA 94062

Dr. Clarence R. Mehl
Sandia National Laboratories
Division 7112
P.O. Box 5800
Albuquerque, NM 87185

Jackie Meeks
Lawrence Livermore National Laboratory
University of California
P.O. Box 808, L-90
Livermore, CA 94550

Carol A. Meier
Lawrence Livermore National Laboratory
University of California
P.O. Box 808, L-90
Livermore, CA 94550

Camille Minichino
Lawrence Livermore National Laboratory
University of California
P.O. Box 808, L-91

Mr. Joseph E. Minor
Texas Technological College
Lubbock, TX 79408

Andrew Mark
Ballistic Research Laboratory
Attn: DRDAR-BLT
Aberdeen Proving Ground, MD 21005

Robert G. McKee, Jr.
Staff Engineer/Program Manager
Los Alamos Technical Associates Inc.
P.O. Box 410
Los Alamos, NM 87544

Mr. H.L. Murphy
H.L. Murphy, Associates
P.O. Box 1727
San Mateo, CA 94401

National Council on Radiation
Protection and Measurements
7910 Woodmont Avenue
Bethesda, MD 20014

National Fire Protection
Association Library
Batterymarch Park
Quincy, MA 02269

Dr. Fred Offensend
SRI International
333 Ravenswood Avenue
Menlo Park, CA 94025

Thomas Y. Palmer
SWETL Incorporated
P.O. Box 278
Fallbrook, CA 94025

Ron Pape
IIT Research Institute
10 West 35th Street
Chicago, IL 60616

Prof. R.K. Pefley
University of Santa Clara
Santa Clara, CA 95053

Robert F. Perret
Lawrence Livermore National
Laboratory
University of California
P.O. Box 808, L-10
Livermore, CA 94550

Mr. Laurence Pietrzak
Mission Research Corporation
P.O. Drawer 719
Santa Barbara, CA 93102

Mr. William Parker
National Bureau of Standards
Building 224 - Room A-345
Washington, DC 20234

Mr. John Rempel
Center for Planning and Research
2483 East Bayshore, Suite 104
Palo Alto, CA 94303

Thomas A. Reitter
Lawrence Livermore National
Laboratory
University of California
P.O. Box 808, L-140
Livermore, CA 94550

Harvey G. Ryland
Ryland Research, Inc.
5266 Hollister Ave. - Suite 324
Santa Barbara, CA 93111

Martin Rosenbblatt
California Research & Technology,
Incorporated
20943 Devonshore Street
Chatsworth, CA 91311

Mr. John Rockett
National Bureau of Standards
Center for Fire Research Building
Building 224 - Room B-260
Washington, DC 20234

Mr. Fred Sauer
Physics International Company
2700 Merced Street
San Leandro, CA 94577

Dr. Don Scheuch
430 Golden Oak Drive
Protola Valley, CA 94025

Mr. Phillip M. Smith
Associate Director
Natural Resources & Comm. Services
Office of Science and Technology
Policy
Executive Office Bldg.
Washington, DC 20500

Dr. Lewis V. Spencer
National Bureau of Standards
Center for Radiation Research
Building 245 - Room C-313
Washington, DC 20234

Dr. Vilhelm Sjolin
Director of BRADFORSK
The Swedish Fire Research Board
S-115 87 Stockholm, SWEDEN

Mr. Leo Schmidt
Institute for Defense Analyses
Program Analysis Division
1801 N. Beauregard Street
Alexandria, VA 22311

Dr. Ben Sussholz
R1/2094
TRW
One Space Park
Redondo Beach, CA 90278

Dr. Ing. P.G. Seeger
Forschungsstelle fur
Brandschutztechnik
University of Larlsruhe (TH)
75 Karlsruhe 21
Postfach 63380, WEST GERMANY

Dr. Donald Sachs
Kaman Sciences Corp.
1911 Jefferson Davis Highway
Arlington, VA 22202

Mrs. Ruth Schnider
Center for Planning and Research
Inc.
2483 East Bayshore, Suite 104
Palo Alto, CA 94303

Bahaaeldin I. Shehata
U.S. Army, Aberdeen Proving Ground
Terminal Ballistic Division
Aberden Proving Ground, MD 20115

Shyam Shukla
Lawrence Livermore National
Laboratory
University of California
P.O. Box 808, L-90
Livermore, CA 94550

T.R. Slawson
USAE Waterways Experiment Station
(WEST)
Vicksburg, MS 39180

Richard D. Small
Pacific-Sierra Research Corp.
12340 Santa Monica Boulevard
Los Angeles, CA 90025

Brian Stocks
Great Lakes Forest Research Center
P.O. Box 490
Sault Ste. Marie
Ontario, CANADA

Mr. Walmer E. Strope
Center for Planning and Research
Inc.
5600 Columbia Pike, Suite 101
Bailey's Crossroads, VA 22041

Department of Fire Technology
Southwest Research Institute
P.O. Drawer 2851D
San Antonio, TX 78284

Mr. William Taylor
Ballistic Research Laboratories
Aberdeen Proving Grounds, MD 21005
(2 copies)

Henry Tovey
Federal Emergency Management
Agency
National Preparedness Programs
Direcorate
Washington, DC 20472

Gordon Turnbull
Home Office
Scientific Advisory Branch
Horseferry House
dean Ryle Street
London SWIP 2AW, ENGLAND

The Information Center
Forest Fire Research Institute
331 Cooper Street
Ottawa Ontario K1A 043, CANADA

Technology & Management Consultant
330 Washington Street
Suite 613
Marina del Rey, CA 90291

Mr. Thomas Waterman
IIT Research Institute
10 West 35th Street
Chicago, IL 60616 (2 copies)

Dr. Forman Williams
Department of the Aerospace
and Engineering Sciences
University of California
San Diego
La Jolla, CA 03027

Mr. Carl Wiehle
Defense Intelligence Agency
Attn: WDB-4C2
Washington, DC 20301

Mr. C. Wilton
Scientific Service Inc.
517 East Bayshore Drive
Redwood City, CA 94060
(2 copies)

S.C. Woodson
USAE
Waterways Experiment Station (WES)
Vicksburg, MS 39180

J. Worden
USAE Huntsville Division
P.O. Box 1600
Huntsville, AL 35807

J.V. Zaccor
Scientific Service Inc.
517 East Bayshore Inc.
Redwood City, CA 94060

Secretarire d'Administration
Minstere de l'Interieur
Direction General de la Protection
Civile
rue de Louvain, 1
1000 Brussels, BELGIUM

Canadian Defense Research Staff
ATTN: Dr. K.N. Ackles
2450 Massachusetts Ave., NW
Washington, DC 20008 (4 copies)

Director
Civilforsvarsstyrelsen
Stockholmsdage 27
2100 Copenhagen O, DENMARK

Director de la Secuite Civile
The Head of Sivolforsvaret
18 Rue Ernest Cognac
92 Levallois
Paris, FRANCE

Bundesministerium des Innern
Graurheindorfer Strasse 198
5300 Bonn 1, WEST GERMANY

Almannavarnir Rikisins
Reykjavik, ICELAND

Stato Maggiore Difesa Civile
Centro Studi Difesa Civile
Rome, ITALY

Civil Emergency Planning
Directorate
North Atlantic Treaty Organization
1110 NATO
BELGIUM

Jefe, Seccion de Estudios y
Planification
c/Everisto San Miguel, 8
Madrid-8, SPAIN

Ministero dell Interno
Direzione Generale della Protezione
Civile
00100 Rome, ITALY

Directeur de la Protection Civile
Ministere de l'Interieur
36 fue J.B. Esch
Grende-Duiche de Luxembourg

Directeur Organisatie
Bescherming Bevoling
Ministry of Interior
Sachedeldoekshaven 200
Postbus 20011
2500 The Hague, NETHERLANDS

Ministere de l'Interieur
Sandakerveien 12
Postboks 8136
Oslo dep
Oslo 1, NORWAY

Civil Defense Administration
Minitry of Interior
Ankara, TURKEY

Home Office
Home Defense Research Section
Scientific Research and Development
Horseferry House
Dean Ryle Street
London SWIP 2AW
ENGLAND

END

FILMED

1-84

DTIC